UNIVERSYITY OF BUCHAREST
FACULTY OF CHEMISTRY

DOCTORAL THESIS ABSTRACT
COMPLEXES WITH AZOMETHINE DERIVATIVES OF DIAMINES AND DIKETONES

Ph.D. student:
IONELA STAN(ALAN)

Supervisor:
Scientific Ph.D.
Prof.dr. ANGELA KRIZA

2014

COMPLEXES WITH AZOMETHINE DERIVATIVES OF DIAMINES AND DIKETONES

The Schiff bases are versatile ligands for the metal ions, forming stable complexes, which are studied by the coordination chemistry. Schiff bases can act as bidentate, bis-bidentate, tridentate, tetradentate, and multidentate ligands according with the number of the donor atoms and as result the corresponding complexes may be mononuclear, dinuclear or polynuclear respectively. The stereochemistry of the complexes depends on several factors such as the nature of the metal atom, the donor strength, the symmetry of ligands field as well as the working conditions. Because of their coordination ability, the Schiff bases are used as complexing agents and as reagents in the spectrophotometric analysis of metallic ions respectively. The Schiff bases and their complexes are used as catalysts in several industrial chemical or petrochemical processes [1].

The complexes derived from Schiff bases have a special importance due to their structural diversity and their biological involvements. The use of Schiff bases in the medical field is based on their ability to interact with microorganisms (bacteria and fungi) causing diseases. Complexes with base Schiff ligands have many applications in obtaining structural models for metal–enzymes involved in redox biological processes like dioxygen activation, hydrogen peroxide decomposition, or several hydrolytic processes. According to the literature, there are many studies concerning antibacterial, antifungal, antimicrobial, anticonvulsive, anti–HIV, anti–inflammatory and antitumor activity of complexes with Schiff bases [2].

A new field of applications is consistent with fabrication of materials with special optical properties, due of the optical properties such thermochromism and photochromism characteristic for some Schiff bases. Because of these characteristics, this type of compounds was used for the control and the measurement of radiations, for display systems and for optical memory systems [3].

The symmetric, bis-difunctional Schiff bases with donor atoms at distance inside the molecules may be used as ligands in order to obtain polymer complexes that fix the metallic ions at the both ending-points. This kind of complexes generally has both physical properties of the polymer and chemical properties of the ligand. Some of these characteristic properties are thermal stability, insoluble character in common solvents, and increased number of active centers inside the molecules [4].

OBJECTIVES

- Obtaining the Schiff base ligands derived from di-functional compounds and containing an established number of donor atoms (nitrogen and oxygen)
- The synthesis and characterization of Co(II), Ni(II), Cu(II), Cd(II), and Zn(II) complexes with these ligands
- The physical and chemical characterization and determination of the geometry adopted by these complexes
- The study of some physical properties of ligands and of their complexes
- The determination of the influence of the ligands and the obtained complexes regarding the inhibition of some microorganisms and their adherence at the inert substratum.

CONTENT OF THESIS

The thesis **"Complexes with azomethine derivatives of diamines and diketones"** has as finality the obtaining and characterization of some Schiff bases derived from di-functional compounds and, in the same time, to synthesize the complexes of these Schiff bases with Co(II), Ni(II), Cu(II), Cd(II), and Zn(II) ions. The ligands and the complexes were studied from three perspectives such as redox, biological properties and fluorescence point of view.

The first part of the thesis is dedicated to some literature studies regarding the synthesis and characterization of some Schiff bases, and their compounds as well, which were obtained from aromatic diamines similar to *o*–tolidine and aliphatic diketones, and their complexes respectively. The most important aspects that were taken into account were that concerning physico-chemical characterization, formulation and uses of the studied compounds in several fields of activities.

The original results, which were obtained from our research, are presented in the second chapter of the thesis and refers to the synthesis and characterization of five Schiff bases (three of them being new) that can be classified in two groups:

- Schiff bases obtained by the condensation of *o*–tolidine and aromatic aldehydes, namely salicylaldehyde (H_2L^1), 5–bromo–salicylaldehyde (H_2L^2), 3–methoxy–salicylaldehyde (H_2L^3) and pyridine–2–carbaldehyde (L^4) as in Fig. 1**.**
- Schiff base formed in 2,3–butanedione and 2–aminopyridine condensation (L^5).

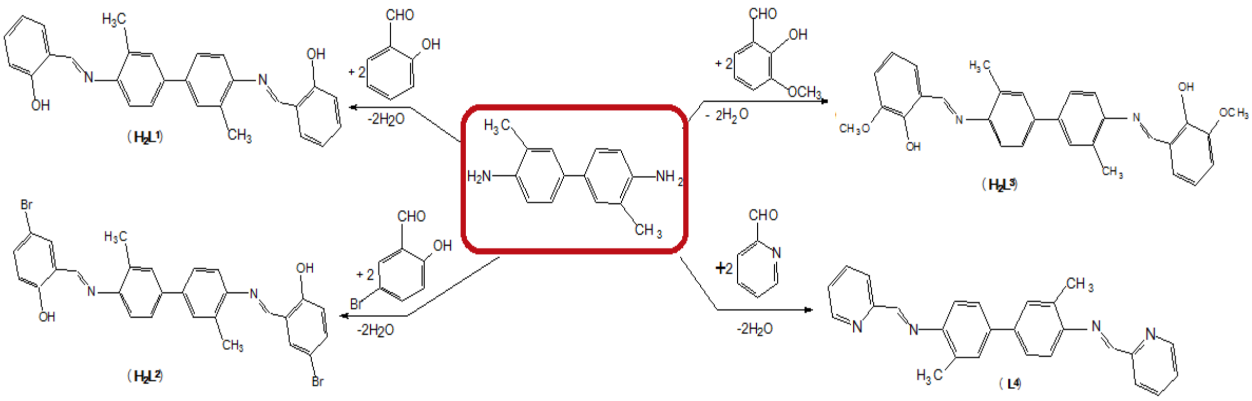

Fig.1. The condensation reaction between *o*–tolidine and some aromatic amines and the obtained ligands

Starting from the divalent ions of transition metals and using the above Schiff bases 59 new complexes were obtained and studied. Also, by the template condensation of butanedione and *o*–phenylenediamine seven new compounds with macrocyclic structure were synthesized. Overall, 66 complexes of Co(II), Ni(II),Cu(II), Cd(II), and Zn(II) ions were synthesized, studied, and characterized.

The complexes were characterized by elemental analysis, IR, UV-Vis, NMR, and EPR (for Cu(II) complexes) spectroscopy, fluorescence spectroscopy, mass spectroscopy (ESI–MS technique), thermal analysis, cyclic voltammetry, antimicrobial activity and influence on adherence to the inert substratum.

The ligands (H_2L) were obtained by condensation reaction from *o*–tolidine with salicylaldehyde, 5–bromo–salicylaldehyde, and 3–methoxy–salicylaldehyde and under controlled pH three types of complexes were synthesized with these Schiff bases:

- Type (I), from 1:1 molar ratio of the ligand and the metal ion that generate binuclear or polynuclear complexes;
- Type (II), for a 1:1 metal : ligand molar ratio, with formation of mononuclear complexes;
- Type (III), when the metal ion and the ligand reacted in a molar ratio 2:1 and it were obtained binuclear complexes.

In the case of the first type of complexes, the ligands act bis-bidentate dianionic similar with the type (III) complexes, while, in the type (II) complexes, the ligand behaves as bidentate monoanionic. Regarding the ligand (L^4), obtained from *o*–tolidine and pyridyl–2–carbaldehyde, this one formed only type (I) and type (III) complexes.

II.1.Complexes of Co(II) and Cu(II) with *N,N'*–bis–(salicyliden)–*o*–tolidine Schiff base

The first chapter of the original part of the thesis describes the synthesis and characterization of the ligand *N,N'*–bis–(salicylidene)–*o*–tolidine (H_2L^1) [5]. Our interest in the condensation product of the *o*–tolidine and salicylaldehyde was focused on the preparation of new complexes that were studied from the perspective of their physico-chemical characterization and biological activity assessment.

The condensation between the *o*–tolidine and the salicylaldehyde is confirmed by the data obtained from the ^{1}H NMR and ^{13}C NMR spectra. At 13.38 ppm, in the ^{1}H NMR spectrum, appears the corresponding signal of the protons from the hydroxyl phenolic groups while the signal of the azomethinic proton appears as a singlet at 8.97 ppm. The ^{13}C NMR spectrum (Fig. 2) shows the characteristic signals of the carbon atoms of both the amine and aldehyde moieties.

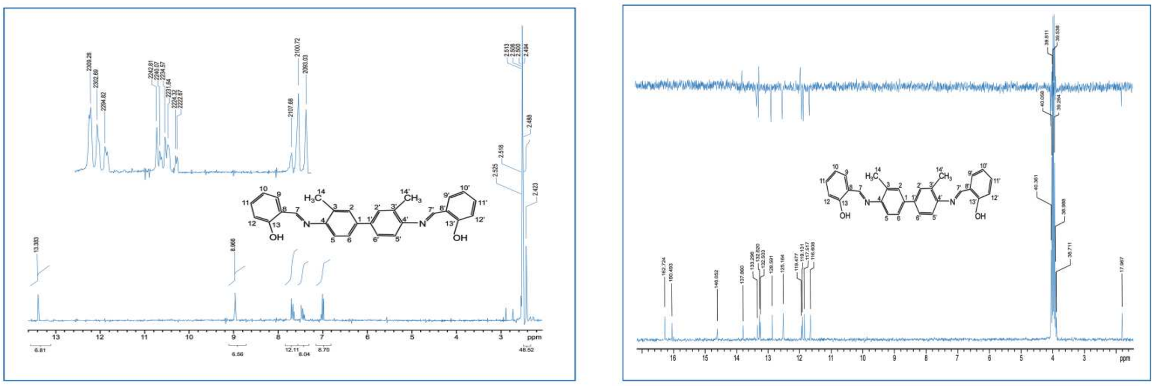

Fig. 2. The ^{1}H NMR and ^{13}C NMR spectra of the ligand (H_2L^1)

The figure 3 presents the mass spectrum recorded for the ligand together with the proposed fragmentation pattern.

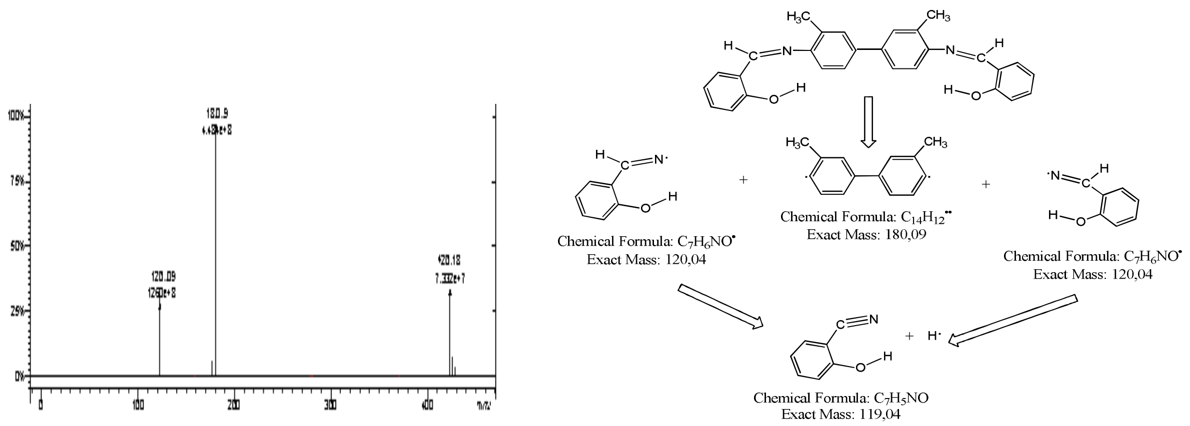

Fig. 3. The mass spectrum of the ligand (H_2L^1) and the fragmentation pattern

Five complexes with 1:1 or 2:1 molar ratio metal–ligand in the presence of triethylamine were obtained. The complexes with formulas $[M_2(L^1)Cl_2(H_2O)_2]$, M = Co(II), Cu(II); $[M(HL^1)X(H_2O)_y]$, M = Co(II), X = CH_3COO, y = 2 ; M = Cu(II), X = Cl, y = 1 and $[Cu(L^1)(H_2O)_2]$ are colored solids, stable at the room temperature, and have a low solubility in the usual organic solvents. The small values of the molar electric conductivity suggest that the complexes are non–electrolytes [6].

The manner by which the ligand (H_2L^1) participated in the coordination process was clarified comparing the ligand IR spectrum with the spectra of the five complexes. However, for the complexes (**1**) $[Co_2(L^1)Cl_2(H_2O)_2]$, (**3**) $[Cu_2(L^1)Cl_2(H_2O)_2]$, and (**4**) $[Cu(L^1)(H_2O)_2]$, the ligand acts as a bis-bidentate in a dianionic form. In the complexes (**2**) $[Co(HL^1)(CH_3COO)(H_2O)_2]$ and (**5**) $[Cu(HL^1)Cl(H_2O)]$, the ligand behaves as bidentate and monoanionic [7].

The electronic spectra of the new five complexes indicate that the metal ions in these complexes have several geometries: octahedral, tetrahedral, or square–planar. These conclusions are confirmed by both the values of the magnetic moments and the values of the crystal field parameters. The small value of 1.28 BM for the calculated magnetic moment of the complex (**4**)$[Cu(L^1)(H_2O)_2]$ suggests a polymeric structure [8].

The powders EPR spectra at room temperature of the Cu(II) complexes confirmed the conclusions about the proposed geometry. In the EPR spectrum of the pseudo–tetrahedral complex (**3**), the shape of the signal is axial with the unpaired electron localized in the d_{xy} orbital (Fig. 4).

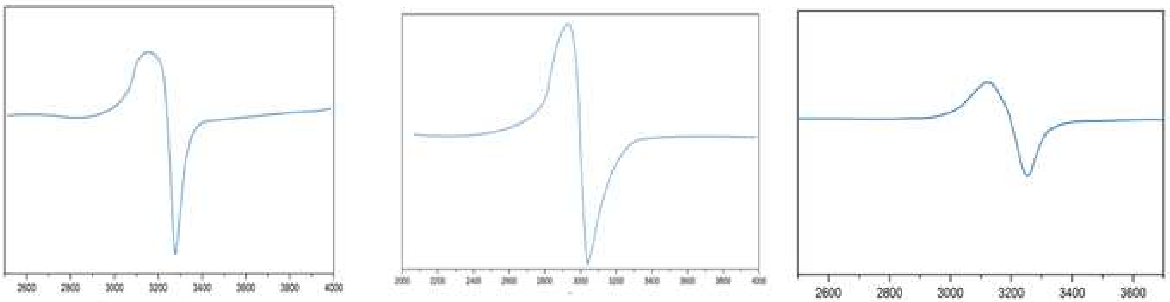

a b c

Fig. 4. Powder EPR spectra of complexes (**3**)-a, (**4**)-b and (**5**)-c

The values of g tensor (g_{II} = 2.217 and $g_{\perp}$ = 2.052) and the geometrical G = 4.05 indicate an increase of the covalent character of the metal – ligand bond and suggest that, in solid state, the change interactions between the two centers of cooper are quite neglected [20] (Fig. 4a). The EPR spectrum of the complex (**4**) shows an isotropic signal (Fig. 4b), strong and broad, without hyperfine splitting, with g_{iso}= 2.080; all these data confirm the octahedral environment of the metallic ion [21]. For the square–planar complex (**5**), the shape of the signal is axial (Fig.4.c), the unpaired electron being located in the d_{x2-y2} orbital, and the ground state being $^2B_{1g}$. The values $g_{II} > g_{\perp} > 2.053$ (2.127 > 2.050) and G = 2.54 suggested an exchange interaction between the cooper(II) ions in solid state at room temperature [9].

By cyclic voltammetry it were studied the redox properties of the complexes and the information provided by the values of $\Delta E_p = E_{pa} - E_{pc}$ indicate the stability of the compounds. The high values of ΔE, which were obtained in the case of the complexes (**3**) and (**5**), indicate the fact that the redox processes involve a high potential and, thus, the compounds will have a good stability [10].

The formulation proposed for complexes (**1**) $[Co_2(L^1)Cl_2(H_2O)_2]$ and (**4**) $[Cu(L^1)(H_2O)_2]$ was also confirmed by the data obtained from the thermal analysis. Using the thermal analysis method, it was observed that in the complex (**1**) there are two molecules of coordination water, similar with the complex (**4**). This fact was confirmed by the mass loss in the first step of the complexes decomposition (Fig. 5a and b) [11].

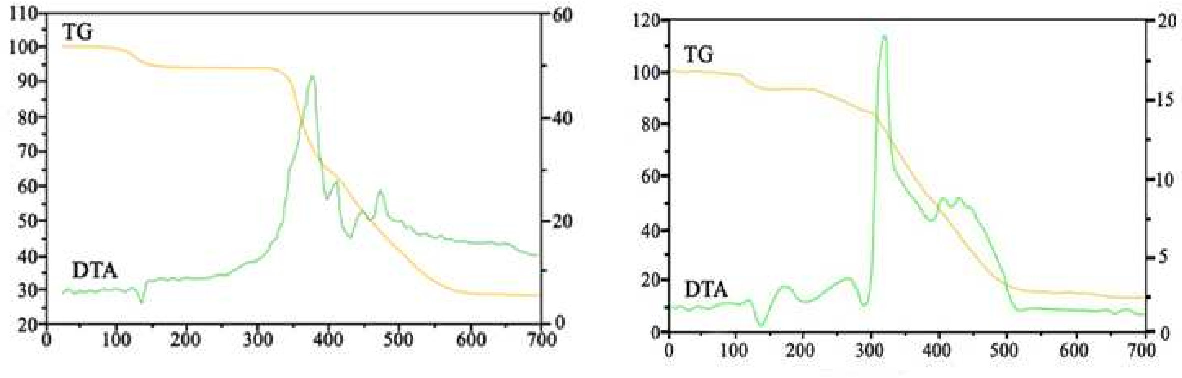

a b

Fig.5. The derivatograms of the complexes (**1**)–a and (**4**)–b

Taking into account the results provided by the elemental analysis, FT–IR, UV-Vis, and EPR spectra well as thermal analyses, the formula presented in figure 6 were proposed for the complexes (**1**) – (**5**).

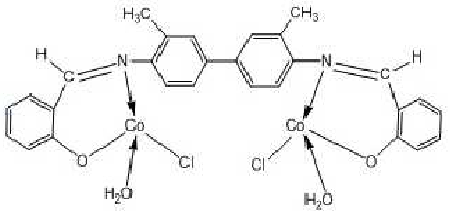

(**1**) $[Co_2(L^1)Cl_2(H_2O)_2]$

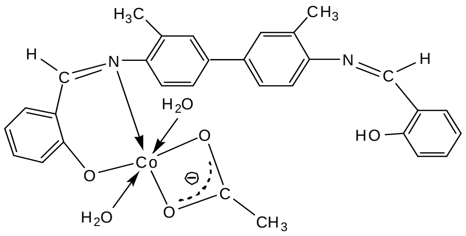

(**2**) $[Co(HL^1)(CH_3COO)(H_2O)_2]$

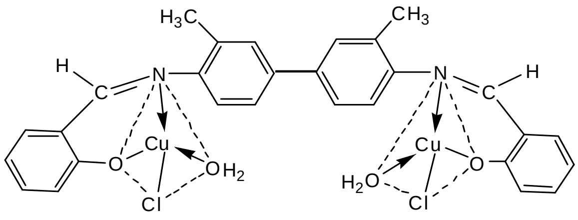

(3) $[Cu_2(L^1)Cl_2(H_2O)_2]$

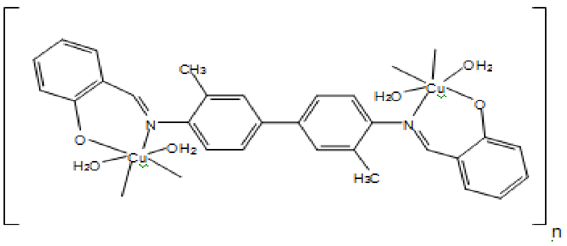

(4) $[Cu(L^1)(H_2O)_2]_n$

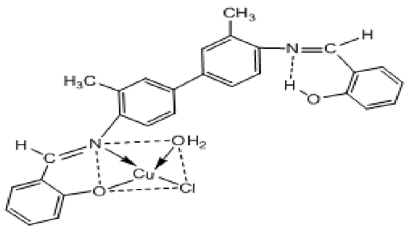

(5) $[Cu(HL^1)Cl(H_2O)]$

Fig. 6. The structural formula proposed for the complexes (**1**) – (**5**)

The ligand (HL^1) and the synthesized complexes (**1**) – (**5**) were tested as well for their antibacterial activity. The results indicate that these compounds have different biological activities against Gram–negative (*Escherichia coli*, *Pseudomonas aeruginosa*) and Gram–positive bacteria (*Staphylococcus aureus*, *Enterococcus faecalis*) respectively in comparison with standard drug Streptomycin was used.

The minimum inhibitory concentrations (MIC in µg/mL) values (Fig. 7) indicate a weak inhibitory activity for the ligand, which increased after complexation.

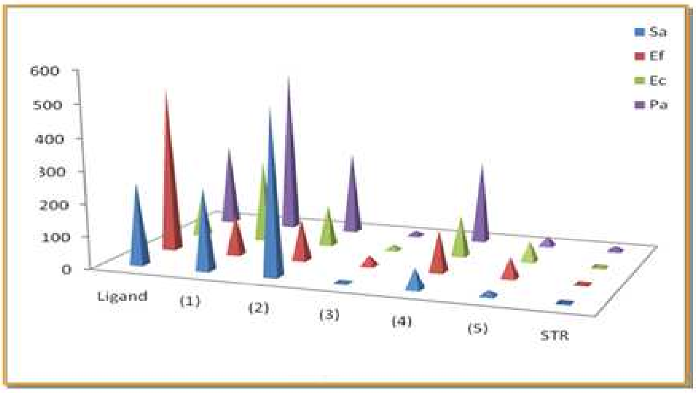

[a] *Sa = Staphylococcus aureus* ATCC 25923*; Ef = Enterococcus faecalis* ATCC 29212
[b] *Ec = Escherichia coli* ATCC 25922*; Pa = Pseudomonas aeruginosa* ATCC 27853, *STR= Streptomicina*

Fig. 7. MIC values (µg/mL) for the ligand (H_2L^1) and the complexes (**1**) – (**5**)

The Cu(II) complexes exhibits a higher inhibitory activity than the Co(II) compounds and it were observed that the tetrahedral complexes were more active than the octahedral ones. The complex (**3**) $[Cu_2(L^1)Cl_2(H_2O)_2]$ exhibits the highest antibacterial activity, but the its MIC values were close and a little bit lower than the Streptomycin values [12].

II.2. Complexes of Co(II), Ni(II), Cu(II), Cd(II), and Zn(II) with *N,N′*–bis(5–bromo–salicilyden)–*o*–tolidine Schiff base

The new ligand *N,N′*–bis(5–bromo–salicilydene–*o*–tolidine) (H_2L^2) was obtained by the condensation of *o*–tolidine with 5–bromo–salicylaldehyde in molar ratio 1:2 [13].

In the IR spectrum of *N,N′*–bis(5–bromo–salicilyden)–*o*–tolidine, appear three characteristic bands at 3444, 1617, and 1176 cm^{-1}, respectively, that can be attributed to the *v*(OH) of the phenol group, *v*(C=N) of the azomethine group and *v*(CO) stretching vibration respectively of the phenolyc group [7,13].

In the ^1H NMR spectrum, the signal of the azomethine proton appears as a singlet at 8.93 ppm and, in the ^{13}C NMR spectrum, the characteristic signal of the azomethine carbon appears at 159.42 ppm.

In the electronic spectrum of the free ligand the absorption bands at 39215 cm^{-1} (255 nm) and 24630 (406 nm) can be attributed to the $\pi \rightarrow \pi^*$ transitions characteristic for the compounds containing benzene rings and C=N bonds [8].

II.2.1 Complexes of Co(II), Ni(II), Cu(II) with *N,N′*–bis(5–bromo–salicilyden)–*o*-tolidine acting as a bis-bidentate form, molar ratio 1:1

The ligand (H_2L^2) behaves similar with ligand (H_2L^1). The complexes are similar with the complex (**1**), but that obtained from (H_2L^2), are: (**6**) $[Co(L^2)]\cdot H_2O$, (**7**) $[Ni(L^2)]$, (**8**)$[Ni(L^2)(H_2O)_2]\cdot H_2O$, and (**9**) $[Cu(L^2)]$. These compounds are polymers, insoluble in all common solvents and melt at higher temperatures. The signals from the mass spectrum of the complex (**6**) $[Co(L^2)]\cdot H_2O$ are according with a polymeric structure (Fig. 8) [14].

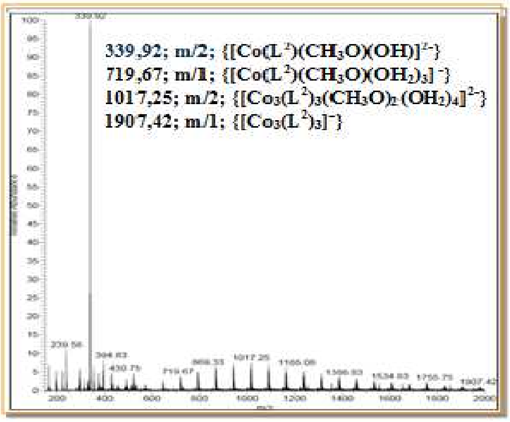

Fig. 8. The mass spectrum of the complex (**6**) together with the assignements for the pseudomolecular ions

In the complex (**6**) [Co(L^2)]·H_2O, the Co(II) ion adopts a tetrahedral geometry, while in the complex (**9**) [Cu(L^2)], the Cu(II) ion has a square–planar one. The Ni(II) ion stereochemistry is tetrahedral in the compound (**7**) and octahedral in (**8**) [Ni(L^2)(H_2O)$_2$]·H_2O respectively (Fig. 9) [8].

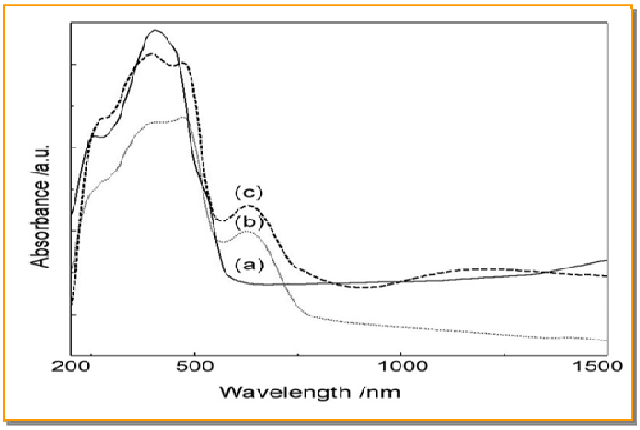

Fig. 9. The UV–vis spectra of the ligand (H_2L^2) – a and complexes (**7**) – b, (**8**) – c

The EPR spectrum of the compound (**9**) is very complex, probably resulting from a superposition of two signals obtained by the decomposition of the main signal. This decomposition can be explained by the existence of two centers with an axial-symmetry. In the figure 10, the obtained signals are presented, as well as the position of the parameters at room and at liquid nitrogen temperature, respectively [9].

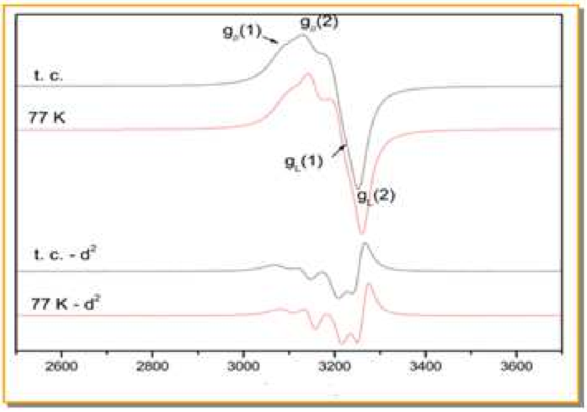

Fig. 10. The powder EPR spectra of the complex (**9**) at room temperature and at 77K, together with the derivate signals (d^2)

The values of the parameters obtained at room temperature, close to those at 77 K, and the values of the geometric parameter G are shown in the Table 1.

Table 1. The values of the spectral parameters for the complex (**9**) at room temperature and at 77 K

Complex (9)	$g_{//}$	$g_{\perp}$	**G**
Room temperature	2.159	2.073	2.17
77K	2.137	2.057	2.40

The thermal studies or these compounds confirm the absence or presence of water as well as its nature, coordination or crystallization water respectively [11]. The high thermal stability of complexes could be an argument for the polymer structures shown in figure 11.

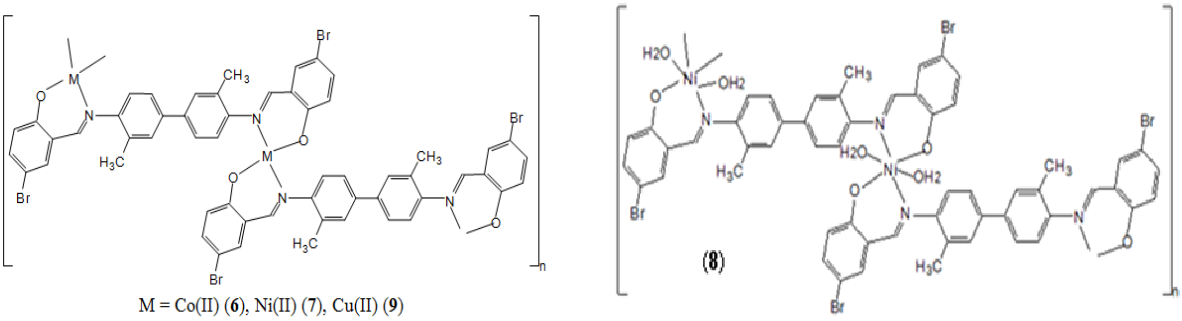

Fig. 11. The structures proposed for the complexes (**6**) – (**9**)

II.2.2 Complexes of Co(II), Ni(II), Cd(II) and Zn(II) with *N,N'*–bis-(5–bromo–salicyliden)–*o*–tolidine acting as bidentate ligand, molar ratio 1 : 1

Using the ligand *N,N'*–bis(5–bromo–salicyliden)–*o*–tolidine (H_2L^2) complexes of type (II) as well, with general formula $[M(HL^2)X(H_2O)_x]_m$, where m = 1, M = Co(II), X = CH_3COO, x = 2 ; M = Ni(II), X = NO_3, x = 2 ; M = Cd(II), X = CH_3COO, x = 0 ; m = 2 M = Ni(II), X = CH_3COO, x = 2 ; M = Zn(II), X = CH_3COO, x = 0 were obtained [13].

The $\Delta\nu$ values calculated from the IR spectral data suggest that in case of acetate complexes, the (CH_3COO) ion acts as bidentate chelate in the complexes (**10**)$[Co(HL^2)(CH_3COO)(H_2O)_2]\cdot 2H_2O$ and (**13**)$[Cd(HL^2)(CH_3COO)]$ or as bridge in the complexes (**12**) $[Ni)_2(HL^2)_2(Ac)_2(H_2O)_4]\cdot 1{,}5H_2O$ and (**14**)$[Zn_2(HL^2)_2(Ac)_2]\cdot 5H_2O$ [7], where Ac = CH_3COO.

The values of the crystal field parameters together with the calculated values of the magnetic moments indicate that in the compounds (**10**)$[Co(HL^2)(CH_3COO)(H_2O)_2]\cdot 2H_2O$, (**11**)$[Ni(HL^2)(NO_3)(H_2O)_2]$ and (**12**)$[Ni_2(HL^2)_2(CH_3COO)_2(H_2O)_4]\cdot 1{,}5H_2O$ the metallic ions have octahedral geometry. For the complexes (**13**)$[Cd(HL^2)(CH_3COO)]$ and (**14**)$[Zn_2(HL^2)_2(CH_3COO)_2]\cdot 5H_2O$ a tetrahedral geometry was proposed by correlating all experimental data [8].

For acetate complexes which contain water molecules, the thermal analysis revealed three decomposition steps, the first one corresponding to the crystallization or coordination water elimination [11]. During the second step, the acetate groups are decomposed into carbonate groups and the bromine is also eliminated while during the last step the ligand is decomposed (Fig.12a and b).

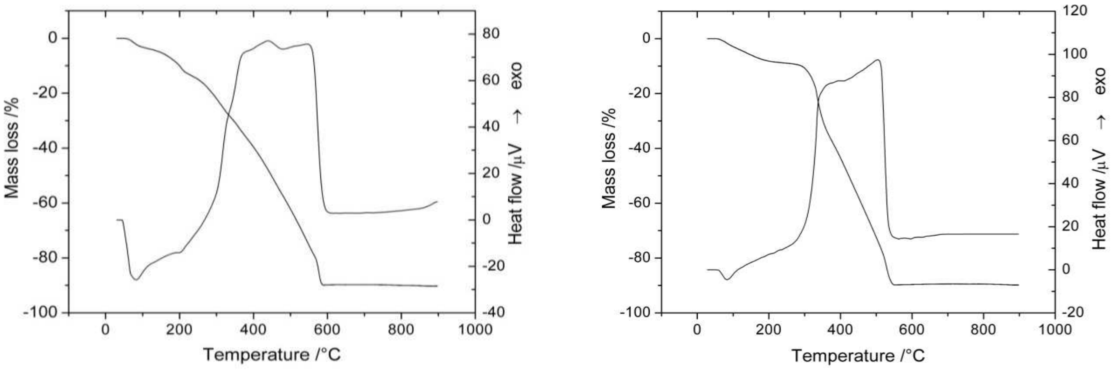

a b

Fig. 12. TG and DTA curves for the complexes (**10**)–a and (**12**)–b

The mass spectrum of the complex (**12**)$[Ni)_2(HL^2)_2(CH_3COO)_2(H_2O)_4]\cdot 1,5H_2O$ argued the existence of the dimeric structure presented in figure 13b and a similar structure was proposed for the complex (**14**) [14]. For the complexes (**10**), (**11**), and (**13**), a monomeric structure was proposed. For example, the figure 13a shows the proposed structure of the complex (**11**) $[Ni(HL^2)(NO_3)(H_2O)_2]$.

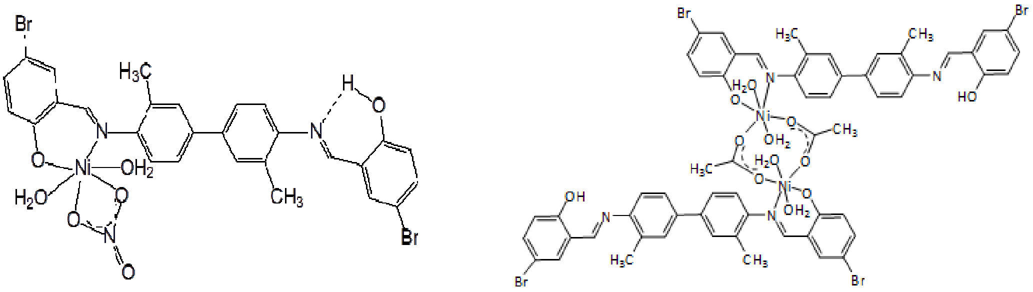

a b

Fig. 13 The structural formula proposed for the complexes (**11**) – a and (**12**) – b

II.2.3. Complexes of Co(II)and Cu(II) with *N,N'*–bis(5–bromine–salicyliden)–*o*–tolidine, acting as bis-bidentate ligand with molar ratio 2 : 1

The spectral studies, molar conductivity measurements, thermal analysis, and elemental analysis indicated for type (III) complexes $[M_2(L^2)(H_2O)_4](ClO_4)_2$, M = Co(II), Cu(II) and $[M_2(L^2)X_2(H_2O)_x]$, M = Co(II), X = NO_3, CH_3COO, x=4 and M= Cu(II), X = NO_3 and CH_3COO, x =0, that at controlled pH, the ligand acts as dianionic bis-bidentate [6,7].

The complexes geometries are presented in Table 2 together with the UV-Vis spectral data [8].

Table 2. UV-Vis spectral data and magnetic moment for (H_2L^2) and complexes (**15**) – (**20**)

Compound	**Absorption maxima**		**Assignments**	**μ/ MB**	**Geometry**
	nm	**cm^{-1}**			
(H_2L^2)	255 406	39215 24630	$\pi \rightarrow \pi^*$	-	-
(**15**) $[Co_2(L^2)(H_2O)_4](ClO_4)_2$	250 375	40000 27030	$\pi \rightarrow \pi^*$	4.17	Tetrahedral
	520	19610	$^4A_2 \rightarrow ^4T_1(P)$		
	680	14700	$^4A_2 \rightarrow ^4T_1(F)$		
(**16**) $[Co_2(L^2)(NO_3)_2(H_2O)_4]$	275 335	36360 29850	$\pi \rightarrow \pi^*$	5.27	Octahedral
	430 520	23255 19230	$^4T_{1g} \rightarrow ^4A_{2g}$ $^4T_{1g} \rightarrow ^4E_g$		
	640	15625	$^4T_{1g} \rightarrow ^4A_{2g}$		
	1195 1485	8370 6735	$^4T_{1g} \rightarrow ^4E_g$ $^4T_{1g} \rightarrow ^4A_{2g}$		
(**17**) $[Co_2(L^2)(CH_3COO)_2(H_2O)_4]$	270 420	37040 23810	$\pi \rightarrow \pi^*$	5.40	Octahedral
	515	18690	$^4T_{1g} \rightarrow ^4T_{1g}(P)$		
	1090	9175	$^4T_{1g} \rightarrow ^4T_{2g}$		
(**18**) $[Cu_2(L^2)(H_2O)_4](ClO_4)_2$	250 420	40000 23810	$\pi \rightarrow \pi^*$	1.56	Tetrahedral
	560	19610	TS L→M		
	720	13890	$d_{z2} \rightarrow d_{x2-y2}$		
(**19**) $[Cu_2(L^2)(NO_3)_2]$	285 410	35090 24390	$\pi \rightarrow \pi^*$	1.96	Tetrahedral
	520	18520	TS L→M		
	700	14290	$d_{z2} \rightarrow d_{x2-y2}$		
(**20**) $[Cu_2(L^2)(CH_3COO)_2] \cdot 2H_2O$	260 425	38460 23530	$\pi \rightarrow \pi^*$	1.85	Tetrahedral
	520	19230	TS L→M		
	715	13990	$d_{z2} \rightarrow d_{x2-y2}$		

By taking into consideration the photochemical properties, the complexes (**9**) $[Cu(L^2)]$, (**10**)$[Co(HL^2)(CH_3COO)(H_2O)_2] \cdot 2H_2O$ and (**11**)$[Ni(HL^2)(NO_3)(H_2O)_2]$ formed by the (H_2L^2), exhibit the same fluorescence, but this is very reduced by the presence of the bromine atom in the molecule of the ligand. In figure 14, it can be observed the absorption (a), excitation – emission (b), and 3D fluorescence spectra for the complex (**9**) $[Cu(L^2)]$.

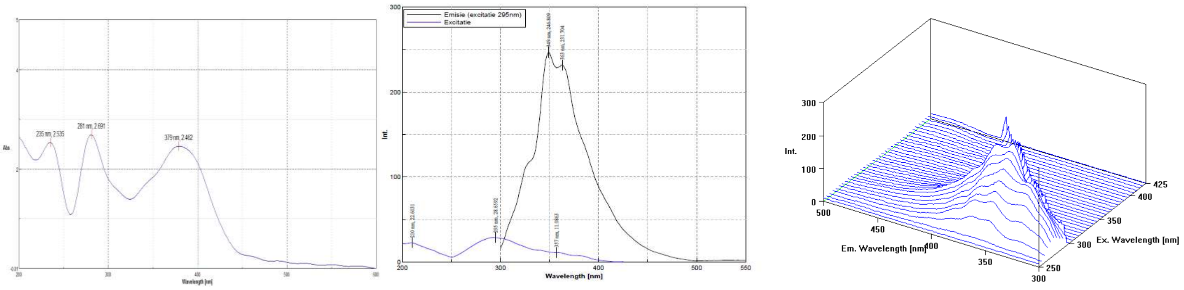

a b c

Fig. 14 The absorption (a), excitation – emission (b), and 3D fluorescence spectra for the complex (**9**) $[Cu(L^2)]$

By comparing the intensity of the issued radiations of the compounds, the minimum fluorescence is observed in the case of complex (**9**) [Cu(L^2)] which it may be explained by his polymer structure. Furthermore, this led to steric impediments, a reduced planarity, and, finally, a reduced fluorescence [15].

The antibacterial activity of the ligand (H_2L^2) and of the corresponding compounds as well as the adherence to the inert substratum was tested using twelve bacterial strains. From these, six were standard strains, while the rest were clinical isolated. It was observed that the inhibition of the bacterial species is different due to the nature of the metallic ion and supports following the order: Co(II) > Ni(II) > Cu(II). The diagram of the MIC (µg/ml) of tested compounds on bacterial strains Gram–positive, Gram–negative, and yeasts is shows in figure 15 [12].

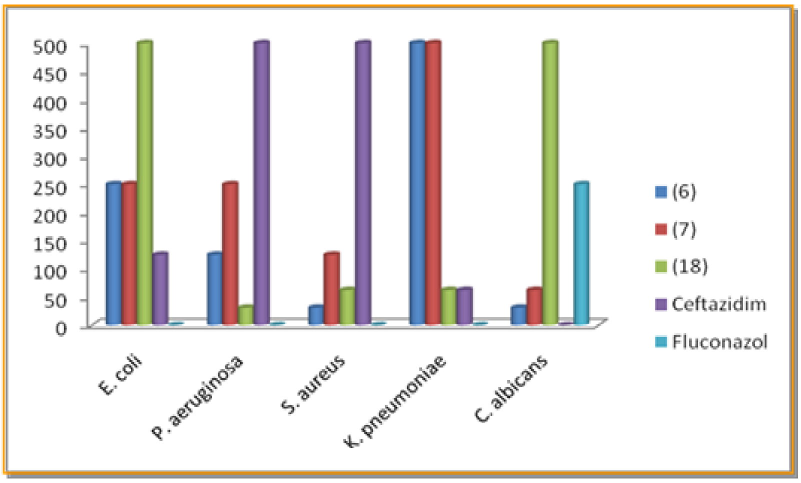

Fig. 15. The MIC values of the complexes (**6**), (**7**), and (**18**) on the tested bacterial strains

The antibacterial activity against the tested species (except for *Klebsiella pneumonia*) is very good in the case of complexes (**6**)) [Co(L^2)]·H_2O, (**7**) [Ni(L^2)], and (**18**)[Cu_2(L^2)(H_2O)$_4$](ClO_4)$_2$, with exceeding the inhibitory capacity of the usual drugs (ceftazidim – CAZ for bacteria and fluconazole – FLZ for fungi). The ligand has a better fungicidal activity than the standard drug, fluconazole.

Concerning the adherence on the inert substratum, the bacterial growth is stopped by the same complexes at minimal inhibitory and subinhibitory concentrations, with more efficiency than ceftazidim – CAZ (standard drug), like in the case of the compound (**18**) [Cu_2(L^2)(H_2O)$_4$]·(ClO_4)$_2$ against *Pseudomonas aeruginosa*.

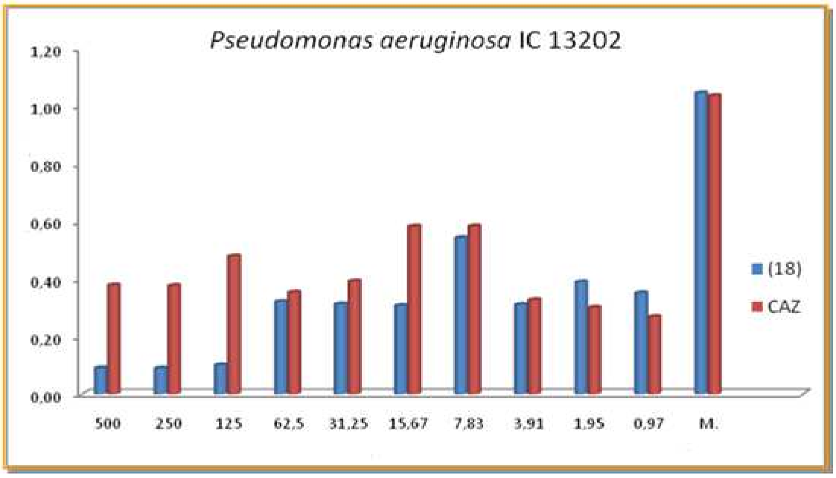

Fig. 16. The study of the influence on the support adherence of the complex (**18**)$[Cu_2(L^2)(H_2O)_4].(ClO_4)_2$ against *Pseudomonas aeruginosa* IC 13202

In the case of fungal strains, the (H_2L^2) ligand favors the decrease of adherence better than fluconazole and studied complexes respectively, especially for the inhibitory concentrations less than MIC (Fig. 17).

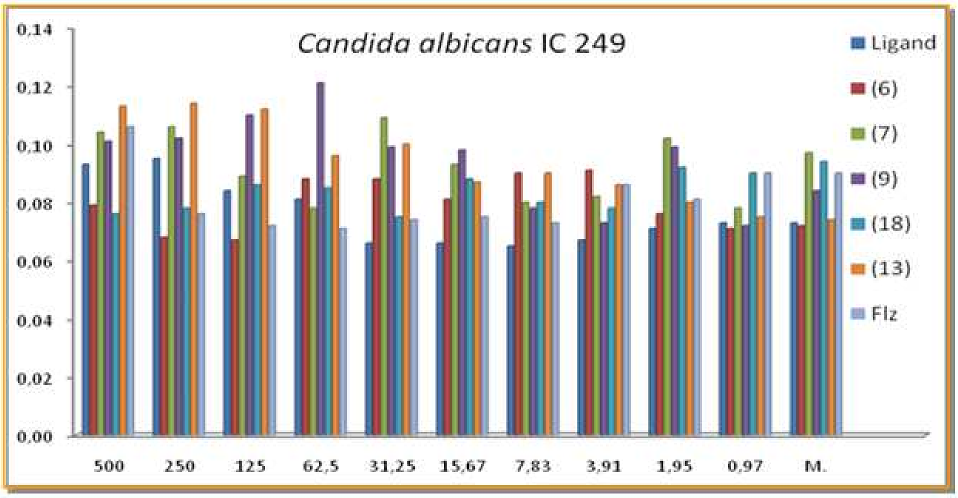

Fig. 17. The study of the influence of the complexes on *Candida albicans* IC 249 adherence

II.3. The complexes of Co(II), Ni(II), and Cu(II) with *N,N'*–bis–(3–methoxy–salicyliden)–*o*–tolidine Schiff base

The ^1H and ^{13}C NMR spectra recorded for the ligand *N,N'*–bis-(3–methoxy–salicyliden)–*o*–tolidine (H_2L^3) have presented the specific signals of the azomethine group. This Schiff base was also obtained as a single crystal which allowed an X–ray diffraction analysis. The ligand crystal structure consists in layers formed by Schiff base molecules. The non–symmetric cell (Fig. 18) contains an irregular molecule (Fragment 1) and a moiety from other molecules; based on symmetry operations, this cell is generating other species more symmetrical (Fragment 2) [16].

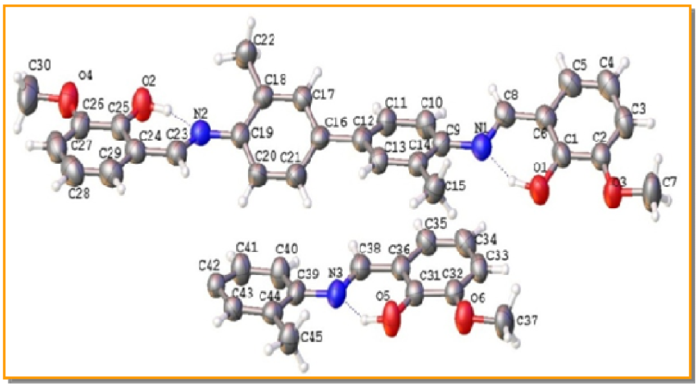

Fig. 18. The basic unit structure of the Schiff base (H_2L^3) and the atom's numbering scheme (with 50% probability of ellipsoid rotation)

All the hydrogen bonds are intramolecular and are formed between phenolic groups and imino groups linking together *o*–vanillin and *o*–tolidine fragments. The packing diagram (Fig. 19) presents the alternative arrangements of a planar molecule which belong to fragment 2 and the two other molecules of the fragment 1. Weak π – π stacking interactions appear between the phenol rings placed in parallel planes from one fragment of the *o*–vanillin and the phenyl ring from the *o*–tolidine fragment.

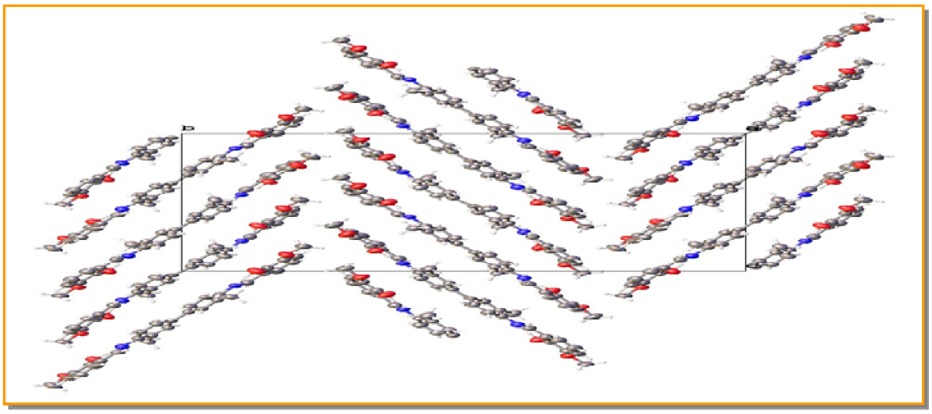

Fig. 19. The packing diagram of the crystalline structure of the compound (H_2L^3) along the axe a

II.3.1.The complexes of Co(II), Ni(II), and Cu(II) with ligand *N,N'*–bis(3–methoxy–salicyliden)–*o*–tolidine, molar ratio 1: 1

At controlled pH values, the ligand (H_2L^3) gives rise to complexes that can be included in three types described above. In the case of complexes (**21**) and (**26**) [$M(HL^3)X(H_2O)$] (M = Co(II), Cu(II)) where the ligand acts monoanionic bidentate, the characteristic band for the azomethine group is split in the IR spectra; this split can be considered as an argument for the coordination mode of this ligand (Table 1 and Fig. 20).

Table 3. IR spectral data (cm^{-1}) for (H_2L^3) and complex (**26**)

Compound	ν(OH)	ν(C=N)	ν(C-O)	$\delta_{(H2O)}$	ν(M-O)	ν(M-N)
(H_2L^3)	3439	1615	1253	-	-	-
(**26**) [$Cu(HL^3)Cl(H_2O)$]	3462	1636 1608	1245	825	561	419

One of these bands is shifted at higher wavenumbers and the other one at lower wavenumbers, in comparison with the ligand spectrum. This allows concluding that only one azomethine group is involved in the coordination while the other remains uncoordinated and is involved in hydrogen intramolecular bond [7].

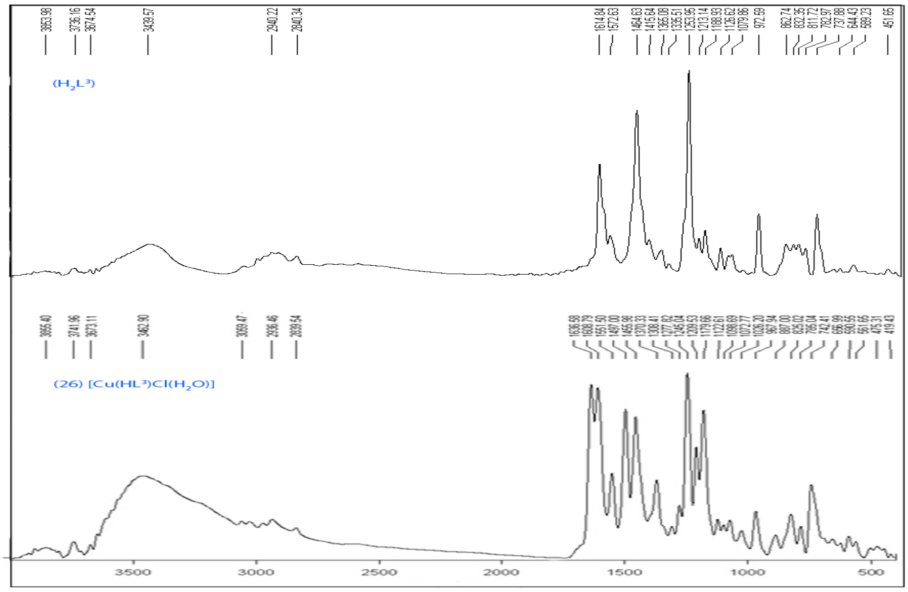

Fig. 20. IR spectra for the Schiff base (H_2L^3) and the compound (**26**)

Some physical data (i.e. the values of the peaks in the mass spectra) indicate a dimeric structure for the complexes (**22**) [$Co(L^3)(H_2O)_2$], (**24**) [$Ni(L^3)(H_2O)_2$], (**27**) [$Cu(L^3)(H_2O)_2$] and a polymeric structure for complexes (**23**) [$Ni(L^3)$], and (**25**) [$Cu(L^3)$] respectively (see Fig. 21) [14].

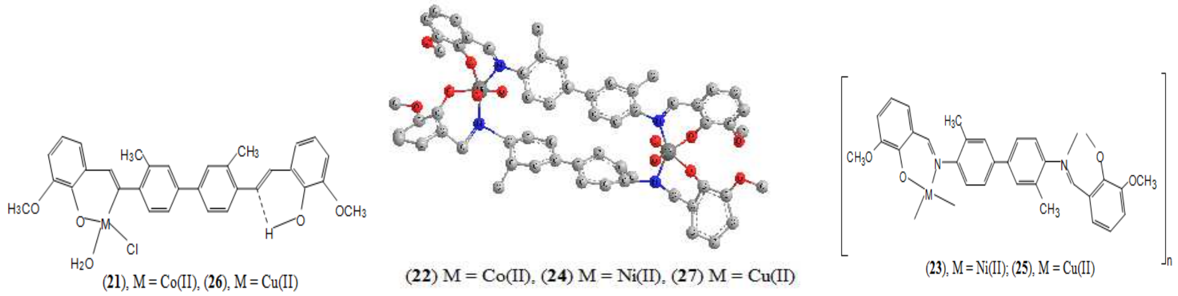

(**21**), M = Co(II), (**26**), M = Cu(II)
(**22**) M = Co(II), (**24**) M = Ni(II), (**27**) M = Cu(II)
(**23**), M = Ni(II); (**25**), M = Cu(II)

Fig. 21. The formula proposed for the complexes (**21**) – (**27**)

II.3.2. Complexes of Co(II), Ni(II), and Cu(II) with N,N'–*bis*–(3–methoxy–salicyliden)–*o*–tolidine Schiff base, molar ratio 2:1

For 2:1 molar ratio metal–ligand the complexes (**28**) – (**31**) were obtained with general formula $[M_2(L^3)(H_2O)_4]X_2$, where M = Co(II), X = ClO_4; M = Cu(II), X = NO_3 and $[M_2(L^3)(CH_3COO)_2(H_2O)_x]$ where M = Co(II), x = 4 and M = Cu(II), x = 0. In all these complexes, the ligand acts as dianionic bis-bidentate [17]. The complexes have tetrahedral geometries except for compound (**29**)$[Co_2(L^3)(CH_3COO)_2(H_2O)_4]$ which exhibits an octahedral environment around the central metallic ion [8]. The thermal analysis confirmed the presence of coordination water in the case of complex (**29**)$[Co_2(L^3)(CH_3COO)_2(H_2O)_4]$ and the existence of crystallization water for the complex (**31**)$[Cu_2(L^3)(CH_3COO)_2]\cdot H_2O$ [11].

The EPR spectra for the Cu(II) complexes with the ligand (H_2L^3) were recorded on powder at room temperature and at 77K and was observed that the geometries are not disturbed by cooling. For example, for the compounds with a distorted geometry the signals were asymmetric and broader in the low field range indicating an orthorhombic symmetry (Fig. 22).

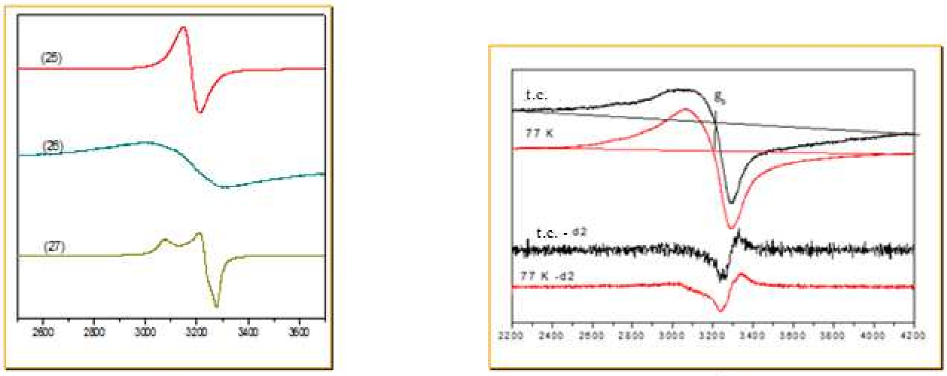

a b

Fig. 22. The EPR spectra (powder) of the complexes (**25**) $[Cu(L^3)]$, (**26**) $[Cu(HL^3)Cl(H_2O)]$, (**27**)$[Cu(L^3)(H_2O)_2]$ – a and (**31**) $[Cu_2(L^3)(CH_3COO)_2]\cdot H_2O$ – b

In order to evaluate the redox properties, cyclic voltammetry studies were performed on the ligand, the metallic salt, and the complexes (**25**)$[Cu(L^3)]$, (**26**)$[Cu(HL^3)Cl(H_2O)]$, (**30**)$[Cu_2(L^3)(H_2O)_4](NO_3)_2$, and (**31**) $[Cu_2(L^3)(CH_3COO)_2]\cdot H_2O$. It was observed that the metal ions stabilize the ligand especially in the compounds (**25**), (**30**), and (**31**). In the case of complex (**26**), the metallic ion is reversible reduced and the values of the reduction potential for the ligand and the complex are very close. The complex (**31**) has a weak reduction peak on the cathode branch, which may be due to the steric impediment created by the acetate counter ion from the molecule (Fig. 23) [10].

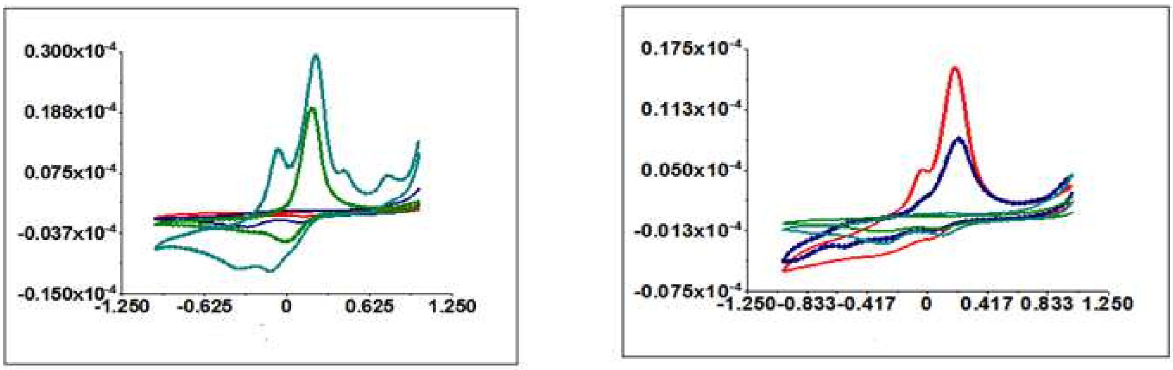

a b

Fig. 23. Voltammograms recorded for the DMSO 10^{-4} M solution of (**25**) $[Cu(L^3)]$ – a (*cyan*) and (**31**) $[Cu_2(L^3)(CH_3COO)_2]\cdot H_2o$ – b (*red*)

For the complexes (**22**)$[Co(L^3)(H_2O)_2]$, (**24**)$[Ni(L^3)(H_2O)_2]$, and (**28**)$[Co_2(L^3)(H_2O)_4](ClO_4)_2$, the fluorescence of the complexes obtained from the ligand (H_2L^2), is higher that the fluorescence due to the presence of group OCH_3. The withdrawing effect of this group induces an increase of electron density on both benzene ring and azomethine group with the increase of the molecule planarity (Fig. 24). It was determined that the light emissions are low for complexes (**22**) and (**24**) with dimeric structure but present high values for complex (**28**) with monomeric structure.

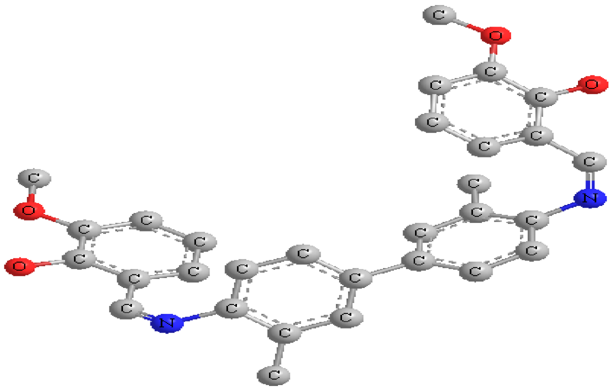

Fig. 24.The molecular pattern of the ligand (H_2L^3)

The antibacterial activity of (H_2L^3) and some of its complexes showed a weak inhibitory ability against Gram–positive and Gram–negative bacteria. In addition to this, they showed a very pronounced activity against fungal strains even higher than fluconazole (Fig. 25).

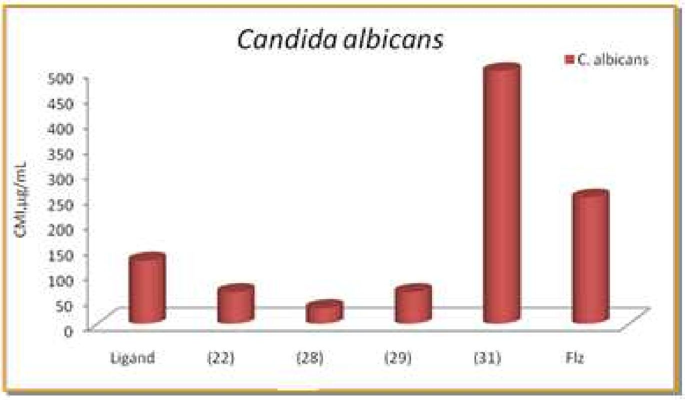

Fig. 25. The MIC values (µg/ml)for the ligand (H_2L^3) and complexes (**22**) [Co(L^3)(H_2O)$_2$], (**28**) [Co_2(L^3)(H_2O)$_4$](ClO_4)$_2$, (**29**)[Co_2(L^3)(CH_3COO)$_2$(H_2O)$_4$], and (**31**)[Cu_2(L^3)(CH_3COO)$_2$]·H_2O against *Candida albicans* strains

We must emphasize the behavior of the complex (**28**) [Co_2(L^3)(H_2O)$_4$](ClO_4)$_2$ which has a MIC value for fungal strains remarkably small (32.5 µg/mL); this compound also prevents much better the growth on substrate at any concentration than the standard drug fluconazole, which makes us conclude that it could be used in practice. Generally, all the compounds were effective against fungi. Moreover, the Co(II) complexes have a very good antifungal activity with MIC values < 62.5 µg/mL [12].

II.4. Complexes of Co(II), Ni(II), Cu(II), Cd(II), and Zn(II) with *N,N'*–bis–(2–pyridylcarbaldehyde)–*o* –tolidine Schiff base

The ligand *N,N'*–bis–(2–pyridylcarbaldehyde)–*o*–tolidine (L^4) was obtained by condensation of pyridine–2–carbaldehyde with *o*–tolidine [18]. The ligand was characterized using the data of the chemical elemental analysis, IR, ^{1}H NMR, ^{13}C NMR and UV-vis spectral data and biological activity.

Complexes of type (I) and (III) were synthesized by using this Schiff base.

II.4.1. Complexes of Co(II), Ni(II) and Cu(II) with *N,N'*–bis–(2–pyridylcarbaldehyde)–*o* –tolidine Schiff base, molar ratio 1 : 1

For type (I) complexes, the formulas are [M(L^4)(H_2O)$_2$]X_2, where M = Co(II), Ni(II), Cu(II) and X = ClO_4; M = Co(II), Ni(II), Cu(II), and X_2 = SO_4 and [M(L^4)X_2], M = Co(II), Ni(II), Cu(II) and X = NO_3, Cl, CH_3COO.

The spectral studies, the data of the thermal analyses, and the values of the molar conductivities show that, in all complexes (**32**) – (**43**), the ligand (L^4) acts neutral bis-bidentate through the azomethine and pyridine nitrogen atoms, while the metal ions addopt an octahedral or a distorted octahedral geometry[7-9].

In the case of the Cu(II) complexes, the spatial arrangement around the central metallic ion is supported by the results of EPR spectroscopy which was recorded both on powder and solution, at room temperature, and at 77 K for the complexes (**40**) $[Cu(L^4)(H_2O)_2](ClO_4)_2$, (**41**) $[Cu(L^4)Cl_2]\cdot 2H_2O$, (**42**) $[Cu(L^4)(NO_3)_2]$, and (**43**) $[Cu(L^4)(H_2O)_2](SO_4)$. The study of the solution was possible due to the good solubility of the above complexes, which is a rare situation for complexes obtained with other ligands derived from *o*–tolidine.

The EPR signal corresponds to a cubic symmetry in the case of the complex (**40**) which was recorded on powder and to an axial symmetry for complexes (**41**) and (**43**) (Fig. 26a). In addition to this, an axial symmetry was also observed for complex (**42**), but the signal is more complex. The reason for this may be the overlap of two signals which appear after analysis of the second derivative of the absorption curve (d^2). This analysis was performed both at room temperature and at 77K (Fig. 26b).

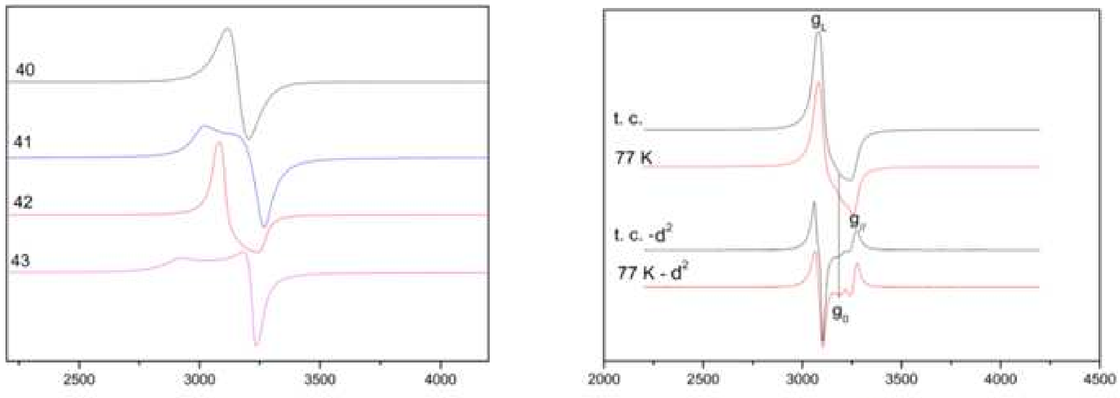

a b

Fig. 26. EPR spectra recorded on powder, at room temperature, for the compounds (**40**) – (**43**) – a, and for the complex (**42**) at room temperature and at 77K – b

After the dissolution in DMSO of the mentioned complexes at room temperature, composed signals was recorded that can be the result of an overlap of two or more signals. This fact is revealed for the complex (**43**) which presents a strong splitting tendency in four hyperfine components. This behavior is typical for centers with a strong tetragonal distortion

(Fig. 27a). At 77K, the recorded signals are simpler and, generally, they correspond to an axial symmetry (Fig. 27b).

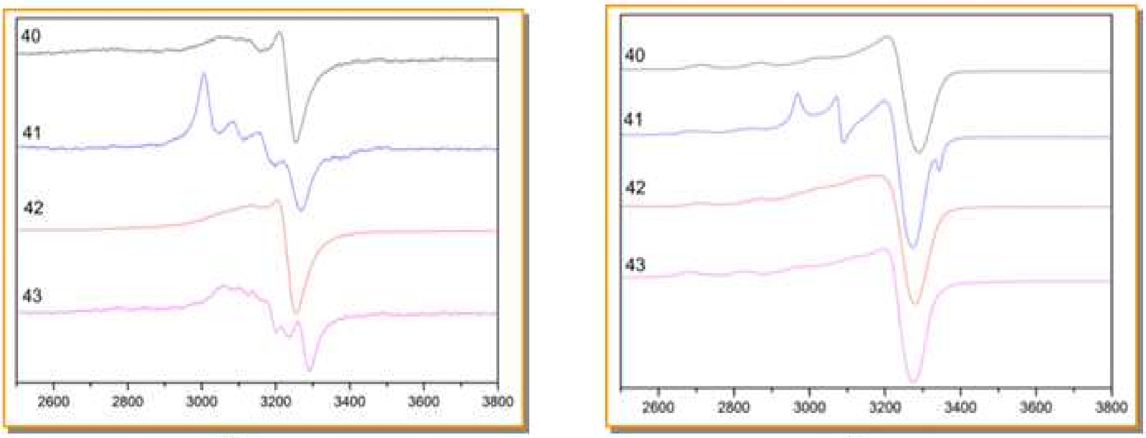

a

b

Fig. 27. EPR spectra recorded in solution for complexes (**40**) – (**43**) at room temperature – a and at 77K – b

The behavior of complex (**41**) was very interesting due to the complexity of the signals which was recorded at room temperature and at 77K (Fig. 28a and b). Thus, their variation in time shows a relative less stability of the complex in solution.

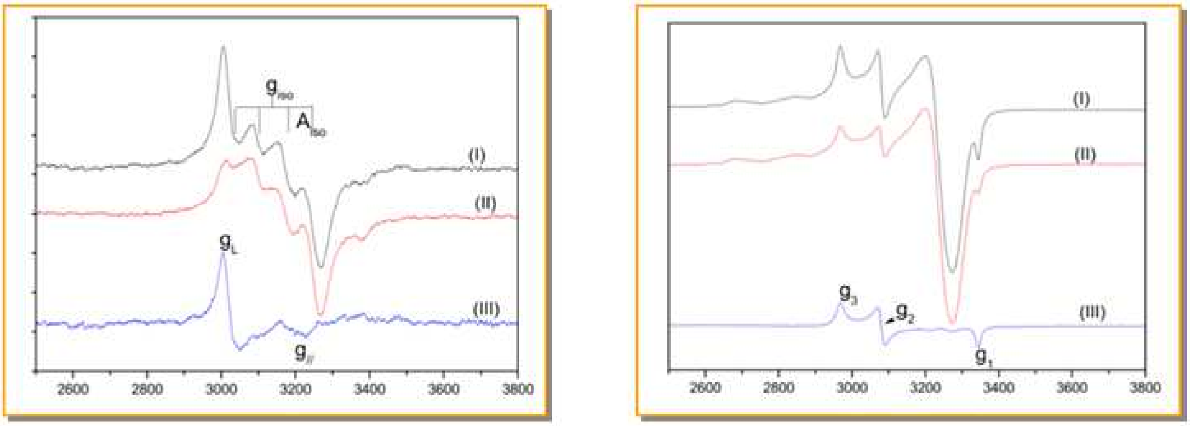

a

b

Fig. 28. The signals of the complex (**41**) at room temperature – a, and at 77K – b:
(I) 27.IX.2011, (II) 05.X.2011, (III) Difference = signal (I) – signal (II)

The mass spectroscopy was performed through the technique of negative electrospray (ESI–MS) for complexes (**40**) $[Cu(L^4)(H_2O)_2](ClO_4)_2$, and (**41**) $[Cu(L^4)Cl_2]\cdot 2H_2O$. The polymeric structure of complexes is supported by the values of the recorded peaks (Fig. 29a and b) which correspond to the negative molecular ions of the polymeric fragment [14].

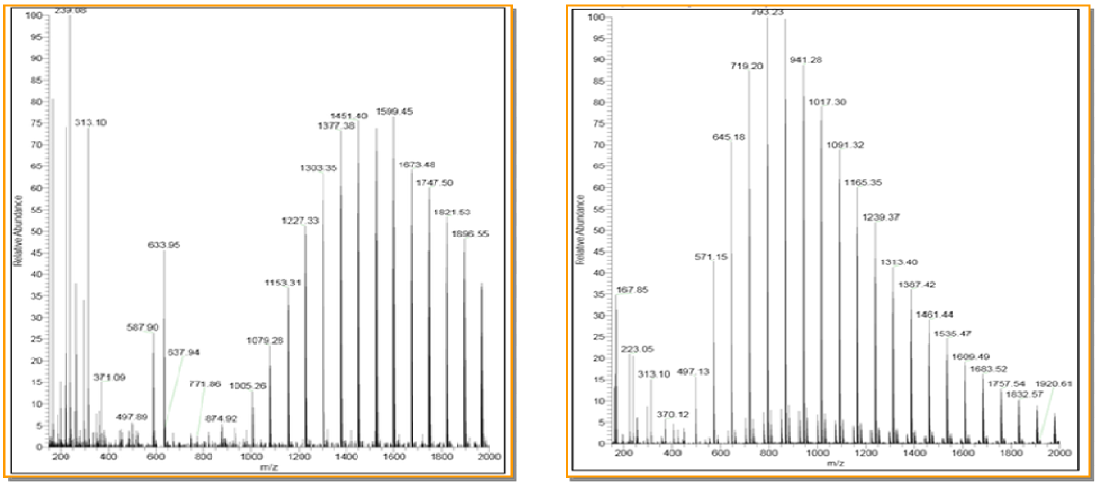

a b

Fig. 29. Mass spectra for the complexes (**40**) – a and (**41**) – b

The structural formulas proposed for the compounds (32) – (43) are presented in Fig.30.

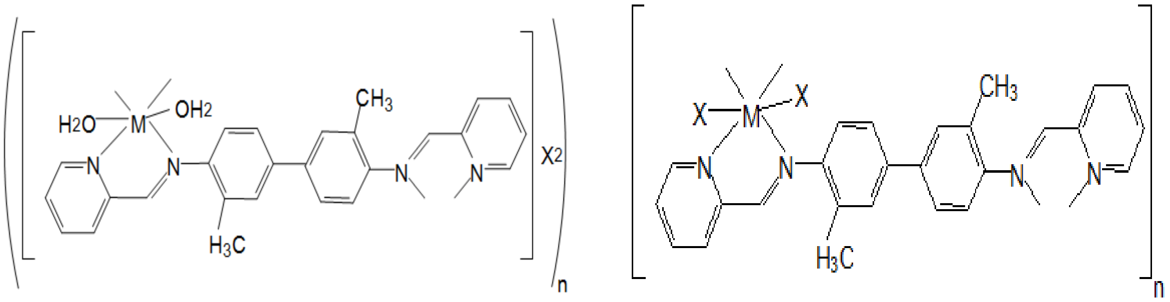

(**32**) M = Co(II), X = ClO_4; (**34**) M = Co(II), X_2 = SO_4;
(**35**) M = Ni(II), X = ClO_4; (**39**) M = Ni(II), X_2 = SO_4;
(**40**) M = Cu(II), X = ClO_4; (**43**) M = Cu(II), X_2 = SO_4

(**33**) M = Co(II), X = CH_3COO;
(**36**) M = Ni(II), X = Cl; (**37**) M = Ni(II), X=NO_3;
(**38**) M = Ni(II), X = CH_3COO;
(**41**) M = Cu(II), X = Cl; (**42**) M = Cu(II), X=NO_3

Fig. 30. The proposed structural formulas for compounds (**32**) – (**43**)

II.4.2. Complexes of Co(II), Ni(II), Cu(II), Cd(II), and Zn(II) with *N,N'*–bis–(2–pyridylcarbaldehyde)–*o*–tolidine Schiff base, molar ratio 2:1

The type (III) complexes with ligand (L^4) have the following formulas: (**44**)$[Co_2(L^4)Cl_4]\cdot H_2O$,(**45**)$[Co_2(L^4)(NO_3)_2(H_2O)_4](NO_3)_2$, (**46**)$[Cu_2(L^4)(Ac)_4(H_2O)_4]\cdot H_2O$, (**47**)$[Cd_2(L^4)Cl_4]$, (**48**)$[Zn_2(L^4)Cl_4]$, (**49**)$[Zn_2(L^4)(NO_3)_2](NO_3)_2$, and (**50**)$[Zn_2(L^4)(Ac)_4]$, where Ac = CH_3COO.

The complexes (**47**) $[Cd_2(L^4)Cl_4]$and (**48**) $[Zn_2(L^4)Cl_4]$ was characterized by the ^{1}H NMR and ^{13}C NMR spectra and, also, by the associated diagrams of ^1H – ^1H COSY and

2D–HECTOR. For example, in the figure 31a and b are presented the ^{1}H NMR and ^{13}C NMR spectra for the complex (**47**) [$Cd_2(L^4)Cl_4$] (Fig. 31a and b).

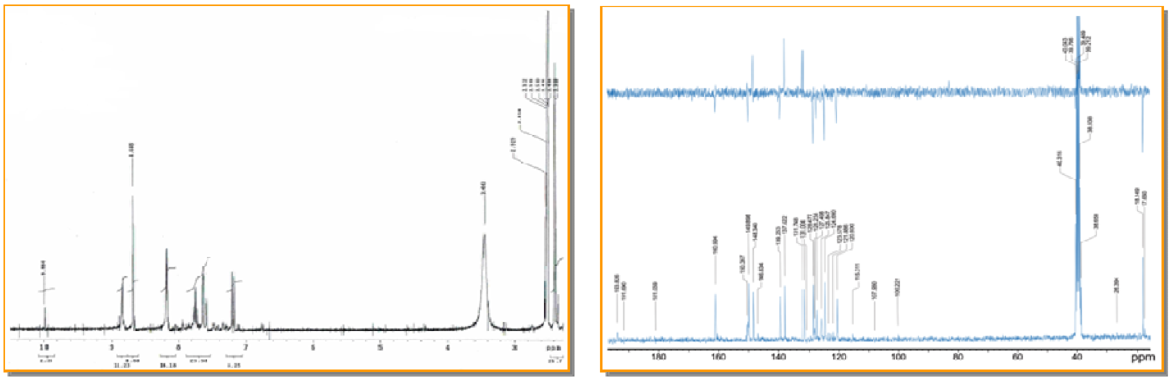

a b

Fig. 31 The ^{1}H NMR – a and ^{13}C NMR – b spectra for the complex (**47**) [$Cd_2(L^4)Cl_4$]

In the structure of the complexes with (L^4) ligand with 2:1 ratio metal : ligand (type (III) complexes), the metal ions addopt a tetrahedral geometry with the exception of the complexes (**45**) [$Co_2(L^4)(NO_3)_2(H_2O)_4](NO_3)_2$ and (**46**) [$Cu_2(L^4)(CH_3COO)_4(H_2O)_4]\cdot H_2O$, where the metal ions have octahedral stereochemistry with a tetragonal distortion. The UV-Vis spectra of the ligand and of the complex (**46**) are comparatively show in figure 32.

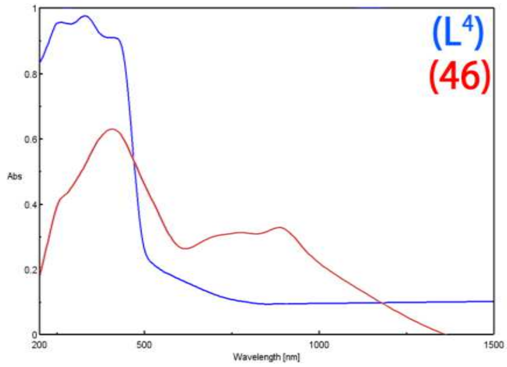

Fig. 32. The UV-Vis spectra of the *N*,*N'*–bis–(2–pyridylcarbaldehyde)–*o* –tolidine ligand (L^4) and of the complex (**46**) [$Cu_2(L^4)(CH_3COO)_4(H_2O)_4]\cdot H_2O$

The spatial arrangement of Cu(II) ion in the complex (**46**) is also confirmed by the powder EPR signal. This signal is characteristic for a cubic symmetry but it is broad and asymmetric (Fig. 33a). If the EPR spectrum is recorded in the compound solution then a complex and overlapped signals are obtained (Fig. 33b and c). In order to study these signals, the second derivative (d^2) analysis is necessary. The complexity of the signals is given by the presence of several centers in the system with different interactions with the nitrogen donor atoms of the ligand [9].

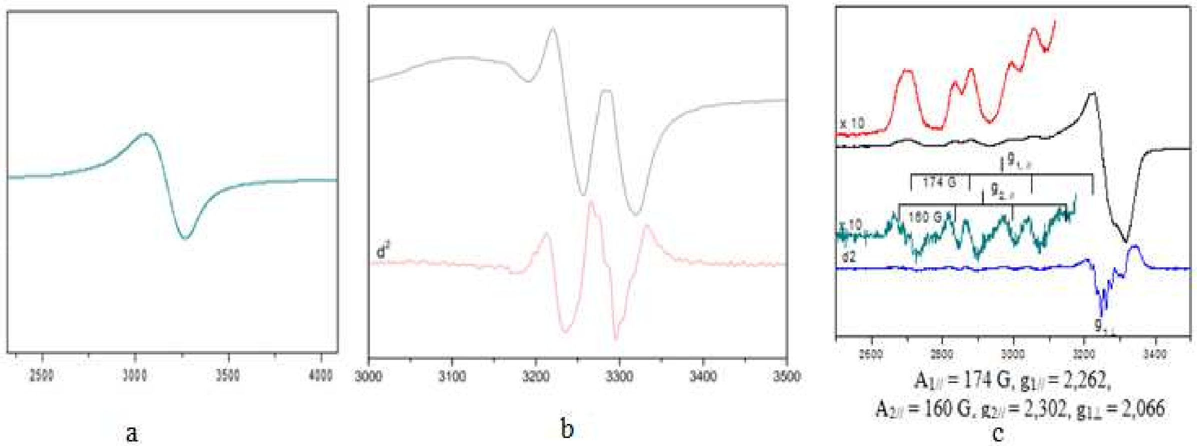

a b c

Fig.33. The EPR spectra of the complex (**46**) recorded on powder – a and in solution, with the (d^2) derivative at room temperature- b and at 77 K - c

Complexes (**32**)$[Co(L^4)(H_2O)_2](ClO_4)_2$, (**36**)$[Ni(L^4)Cl_2]$, and (**46**)$[Cu_2(L^4)(CH_3COO)_4(H_2O)_4]\cdot H_2O$, derived from ($L^4$), present fluorescence, but it is considerably lower than the fluorescence of the complexes with the other ligands. This may be due to the nitrogen atom from the pyridine ring, which has a pair of non–participating electrons that may cause non-radiative transitions. Thus, this may explain the fluorescence diminishing. The fluorescence spectra show that the intensity of the emission for monomer complex (**46**) is higher than the intensity for polymeric complexes, (**32**) and (**36**). It seems that the responsible factor is represented by the very strong steric impediments which appears in this kind of complexes and determines the decrease of the π electrons delocalization [15].

From the qualitative and quantitative antibacterial screening for the (L^4) ligand and for some of its complexes (Fig. 34), it was observed the following: the absence of the activity of the complex (**46**)$[Cu_2(L^4)(CH_3COO)_4(H_2O)_4]\cdot H_2O$, the weak activity of the (L^4) ligand and of the complex (**40**)$[Cu(L^4)(H_2O)_2](ClO_4)_2$, and the good inhibitory ability of complexes (**32**) $[Co(L^4)(H_2O)_2](ClO_4)_2$ and (**44**) $[Co_2(L^4)Cl_4]\cdot H_2O$ [12,18].

The ligand does not have antibacterial activity but instead has fungicidal activity better than fluconazole. Moreover, the tested complexes have antibacterial activity, usually stronger than ceftazidime, but they are not efficient against fungal strains.

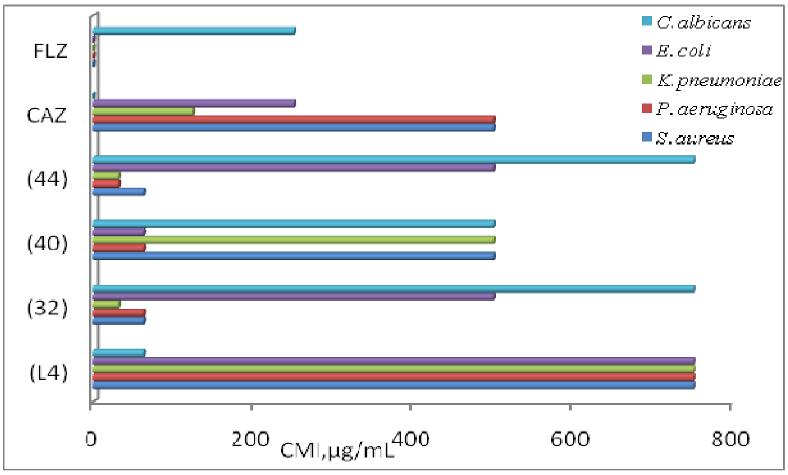

Fig. 34. The MIC values (µg/mL) of (L^4)–ligand, (**32**) $[Co(L^4)(H_2O)_2](ClO_4)_2$, (**40**) $[Cu(L^4)(H_2O)_2](ClO_4)_2$, and (**44**) $[Co_2(L^4)Cl_4]\cdot H_2O$, ceftazidime (CAZ) and fluconazole (FLZ) against the studied microbial strains

In the same context, it was observed that, for all tested complexes, the microorganisms do not adhere to the substrate, especially at minimum inhibitory concentrations, this behavior is sometimes even better than standard drugs (Fig. 35a and b). These observations suggest the possibility of practical application of some complexes as antifungal and even antibacterial agents.

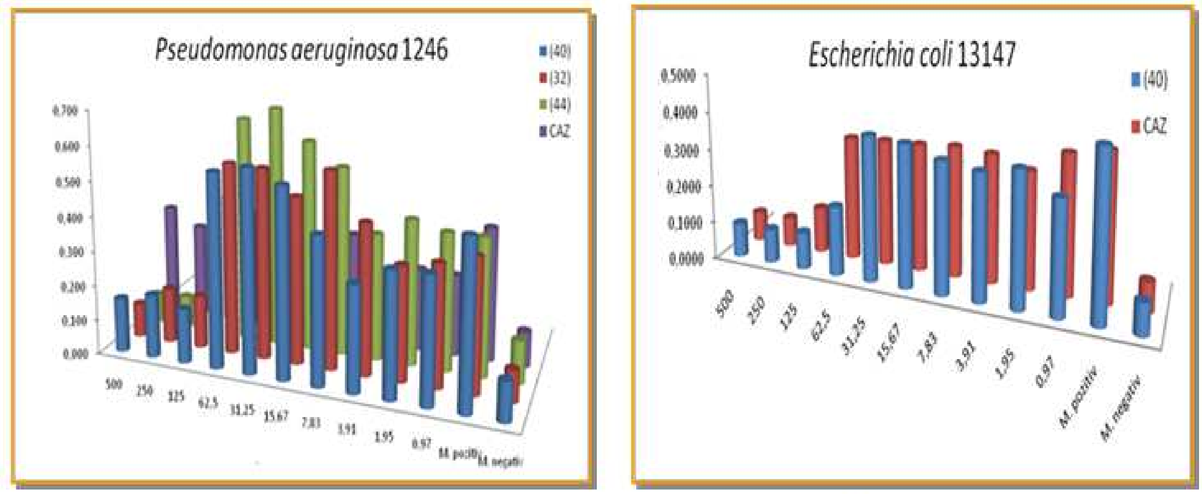

a

b

Fig. 35 The influence of the complex **(40)** $[Cu(L^4)(H_2O)_2](ClO_4)_2$ on the adherence to substrates of the bacterial strains *Pseudomonas aeruginosa* 1246 – a and *Escherichia coli* 13147 – b

II.5. Complexes of Co(II), Ni(II), Cu(II), and Zn(II) with 2–(imino–pyridyl)–3–butanone Schiff base

The second part of the experimental section of the thesis refers to the synthesis and characterization of some ligands derived from butanedione as well as their complexes (Fig.36.).

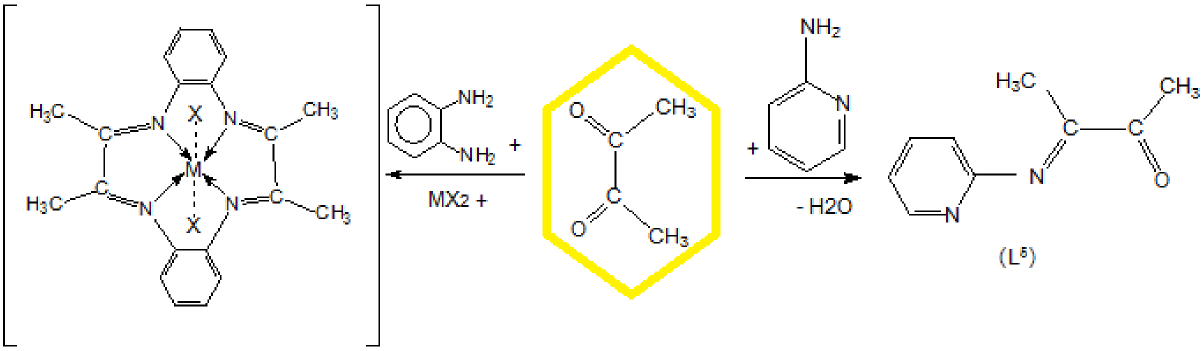

Fig. 36. The reactions of butanedione with aromatic amines

By condensation of the butanedione with 2–amino–pyridine, it was obtained a new ligand, namely 2–(imino–pyridyl)–3–butanone, (L^5), which was characterized by elemental analysis, IR and UV-Vis spectroscopy. By direct reaction involving this ligand or by the template synthesis, it were obtained nine complexes (**51**) – (**59**) using as starting materials some divalent metals salts. These complexes have the following formulas: $[M(L^5)_2(H_2O)_2]X_2$, M = Co(II) or Ni(II), $X_2 = SO_4$; M = Cu(II), X = ClO_4; $[M(L^5)_2X_2]$, M = Cu(II), X = NO_3, CH_3COO; M = Ni(II), X = CH_3COO; $[M(L^5)]Cl_2$ where M = Co(II), Cu(II) and Zn(II).

The data from the IR spectra confirmed the elemental analysis data for the compounds obtained at various molar ratio, namely the fact that in the condensation process only one carbonyl group was involved. The bidentate behavior of the ligand is confirmed by IR data that indicate the fact that the azomethinic nitrogen atom and the oxygen atom from uncondensed carbonyl group are involved in coordination. Unfortunately, the structure of the ligand could not be supported by NMR spectroscopy due to its insolubility in the solvents used for this analysis [7,19].

The electronic spectra and the values of the magnetic moments suggested octahedral geometries for metallic ions, except for the compounds (**52**) $[Co(L^5)_2]Cl_2$ and (**59**)$[Zn(L^5)_2]Cl_2{\cdot}H_2O$ where the metal ion adopt a tetrahedral geometry. The geometry of the complex (**57**) is supported also by the signal present in the EPR spectrum [8,9].

The mass spectra for complexes (**53**) $[Ni(L^5)_2(CH_3COO)_2]\cdot 1,5H_2O$ and (**57**)$[Cu(L^5)_2]Cl_2\cdot 1,5H_2O$ confirmed both their formulas and mononuclear structure (Fig. 37) [14].

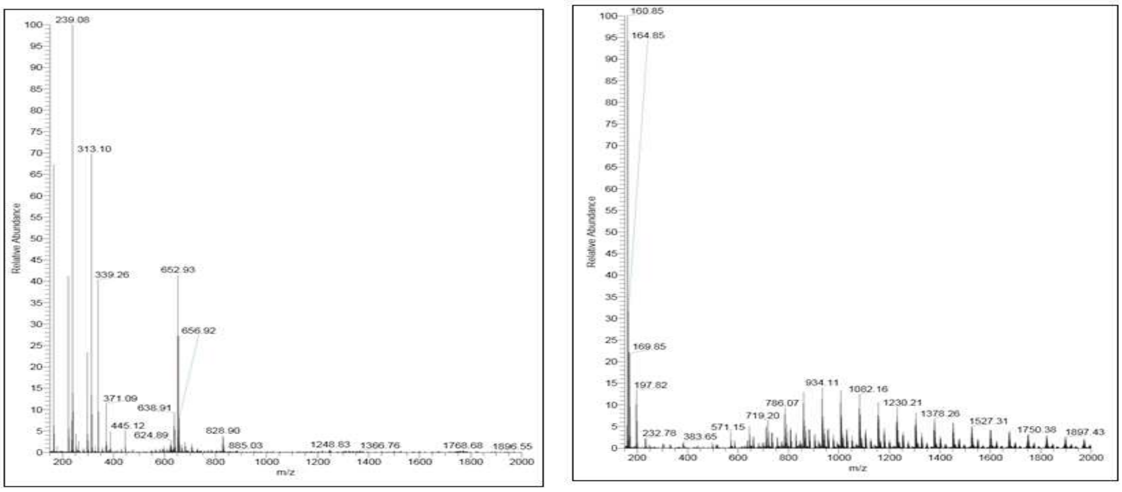

a b

Fig. 37. The mass spectra of the complexes (**53**)$[Ni(L^5)_2(CH_3COO)_2]\cdot 1,5H_2O$ and (**57**) $[Cu(L^5)_2]Cl_2\cdot 1,5H_2O$

The thermal analysis of the complexes with 2–(imino–pyridyl)–3–butanone (L^5) ligand was registered in different conditions [11]. The complexes were decomposed as follows: (**52**) $[Co(L^5)_2]Cl_2$, (**57**) $[Cu(L^5)_2]Cl_2\cdot 1,5H_2O$ and (**59**) $[Zn(L^5)_2]Cl_2\cdot H_2O$ in synthetic air atmosphere and (**51**) $[Co(L^5)_2(H_2O)_2]SO_4\cdot 4H_2O$, (**53**)$[Ni(L^5)_2(CH_3COO)_2]\cdot 1,5H_2O$, (**54**) $[Ni(L^5)_2(H_2O)_2]SO_4\cdot 3H_2O$ and (**58**) $[Cu(L^5)_2(CH_3COO)_2]\cdot 2H_2O$ in nitrogen (Fig. 38a and b).

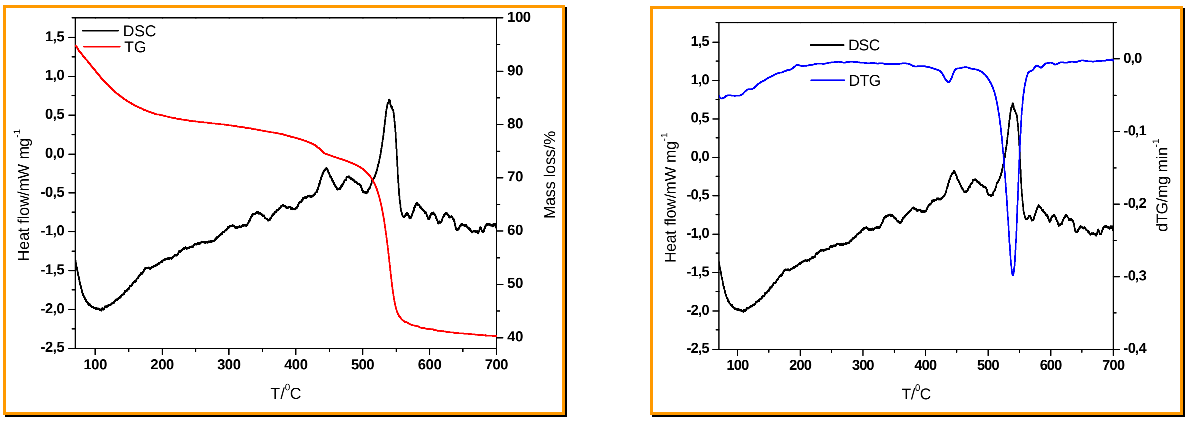

a b

Fig. 38. The thermogravimetric curves of the complexes (**51**) $[Co(L^5)_2(H_2O)_2]SO_4\cdot 4H_2O$: a-TG and DSC, b- DTG and DSC

The data provided by the thermal analysis confirmed either the presence or the absence of the crystallization and/or coordination of water molecules. For the thermal analysis in inert atmosphere, the residual masses were higher than the calculated values, which correspond to the presence of the metals and their oxides. These values have been attributed to the presence of the coal. The DTG curves for the complexes (**51**), (**53**), (**54**) and (**58**), allowed evaluation of the thermal effects of compounds in decomposition steps [11].

For complexes (**51**)–(**59**) the structural formulas presented in the figure 39 were proposed.

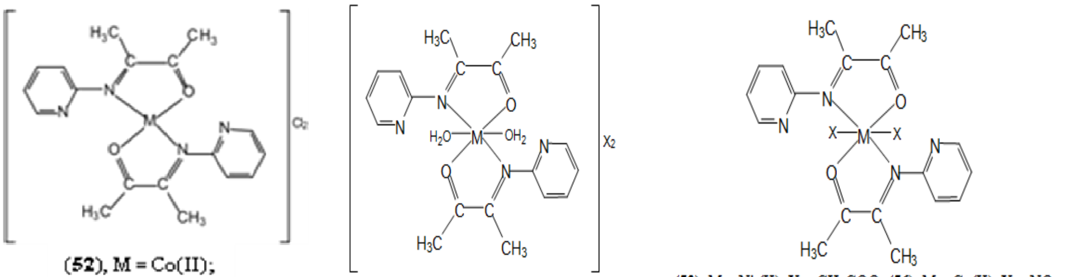

(**52**), M = Co(II);
(**57**) M = Cu(II),
(**59**) M = Zn(II)

(**51**), M = Co(II) , $X_2 = SO_4$; (**54**), M = Ni(II), $X_2 = SO_4$;
(**55**) M= Cu(II), X = ClO_4

(**53**), M = Ni (II), X = CH_3COO; (**56**), M = Cu(II), X = NO_3;
(**58**), M = Cu(II), X = CH_3COO

Fig. 39. The structural formulas proposed for the compounds (**51**)– (**59**)

The antimicrobial tests revealed a weak inhibitory capacity against the Gram–positive and Gram–negative bacteria for the ligand (L^5) and some of its complexes; an exception was the compound (**51**) $[Co(L^5)_2(H_2O)_2]SO_4{\cdot}4H_2O$, which had a pronounced inhibitory activity against the *Pseudomonas aeruginosa* strains (MIC = 62.5 µg/mL) [12]. The Schiff base (L^5) and its complexes (**51**) $[Co(L^5)_2(H_2O)_2]SO_4{\cdot}4H_2O$, (**55**)$[Cu(L^5)_2(H_2O)_2](ClO_4)_2$, and (**56**)$[Cu(L^5)_2(NO_3)_2]$ (Fig. 40) showed instead a fungal activity.

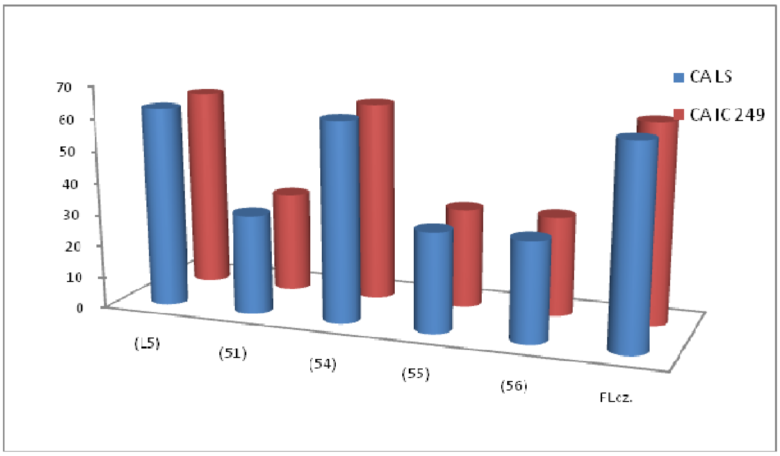

Fig. 40. The MIC values (µg/mL) for ligand (L^5) and some complexes

All the complexes with ligand (L^5) have lower MIC values than fluconazol (Flcz). This indicate the possibility of using them in order to obtain specific drugs. The complex (**54**) $[Ni(L^5)_2(H_2O)_2]SO_4{\cdot}3H_2O$, the ligand ($L^5$), and fluconazol exhibit comparable fungal activity.

The adherence on substrate tests revealed that all complexes decrease the adherence of the fungal strains *Candida* isolated from saliva, at minimal inhibitory concentrations, being much more efficiently than fluconazole (Fig. 41) [12].

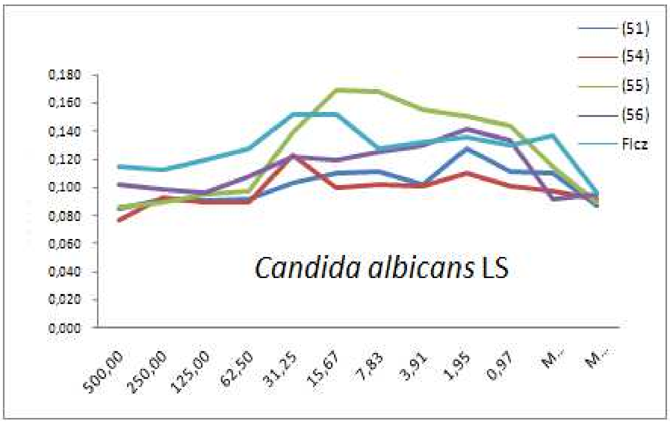

Fig. 41. The reprezentation of the MIC values (µg/mL) of the ligand, complexes and the fluconazol

II.6. Complexes of Co(II), Cu(II), Cd(II), and Zn(II) with macrocyclic Schiff base 2,3,8,9-tetrametildibenzo-[1,4,7,10]tetraazaciclododecina

Due to the lack of references in the literature about compounds with macrocycle structures derived from butanedione, we had the purpose to obtain and to characterize this type of complexes. By performing template synthesis between butanedione and *o*–phenylenediamine, seven complexes (**60**)–(**66**) which have following types formulas were obtained:

$[M(L^6)(H_2O_2)_2]X_2$ where M = Co(II) and Cu(II), X = ClO_4 ; M = Cu(II), X = SO_4

$[M(L^6)X_2]$ where M = Cu(II), X = Cl, CH_3COO

$[M(L^6)(H_2O_2)_x]Cl_2$ where M = Cd(II), x = 0; M = Zn(II), x = 1.

The IR spectra of the synthesized compounds suggested that by template method it were obtained macrocyclic complexes, the ligand (L^6) acting as tetradentate and neutral [20].

The electronic spectra indicated that the metal ions adopt octahedral geometries in complexes, except compounds (**65**) $[Cd(L^6)]Cl_2$ with tetrahedral geometry and (**66**)$[Zn(L^6)(H_2O_2)]Cl_2\cdot 2H_2O$ with square pyramidal geometry. The powder EPR spectra support the proposed geometry for the Cu(II) complexes [8,9].

For the complexes (**64**) $[Cu(L^6)(H_2O_2)_2]SO_4 \cdot H_2O$ and (**66**)$[Zn(L^6)(H_2O_2)]Cl_2$·2H2O it was performed the thermal analysis, in inert atmosphere. The thermogravimetric curves are shown in figure 42.

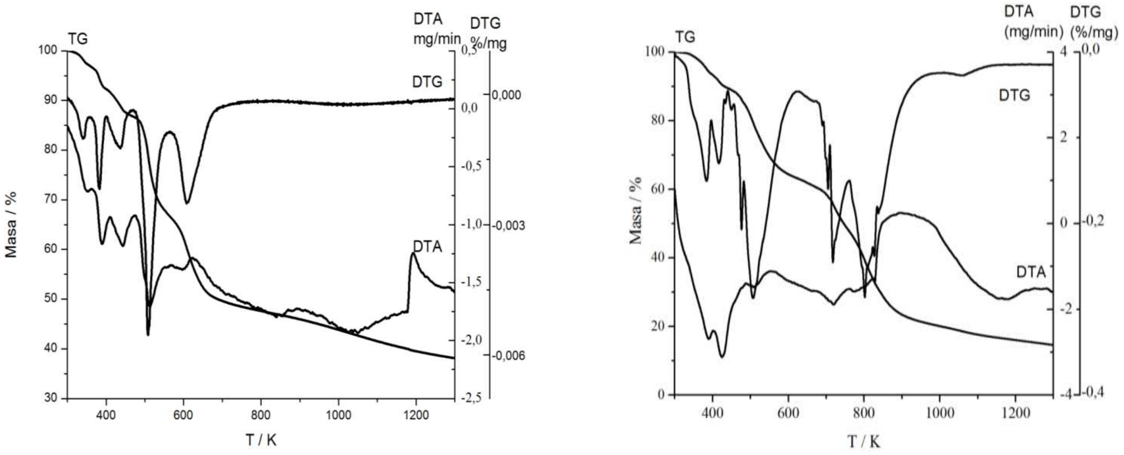

a b

Fig. 42. The thermogravimetric curves for the complexes (**64**) – a and (**66**) – b

Thus, the molecular formulas attributed to the complexes (**62**)$[Cu(L^6)Cl_2]$, (**63**)$[Cu(L^6)(CH_3COO)_2] \cdot H_2O$, (**64**)$[Cu(L^6)(H_2O_2)_2]SO_4 \cdot H_2O$, and (**66**)$[Zn(L^6)(H_2O_2)]Cl_2 \cdot 2H_2O$ were confirmed [11].

In the figure 43 the proposed formulas for compounds (**60**)–(**66**) are presented.

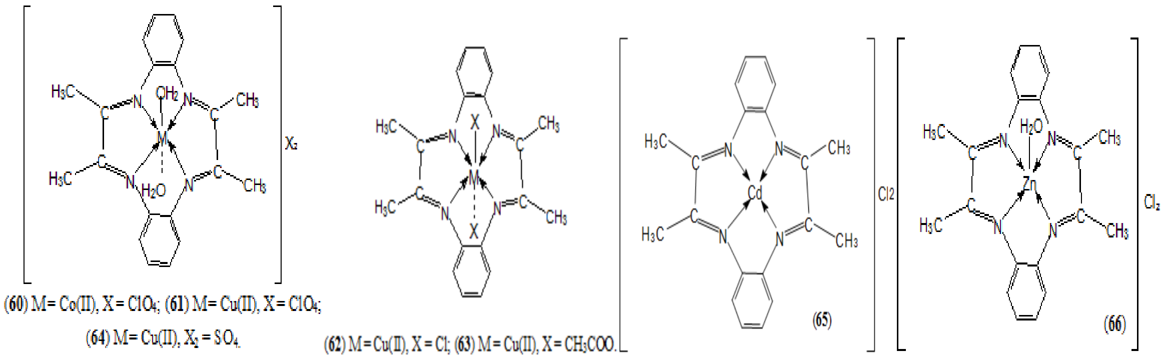

Fig. 43. The proposed formulas for the macrocyclic complexes

The qualitative and quantitative antimicrobial tests were performed for some complexes, namely (**60**) $[Co(L^6)(H_2O)_2](ClO_4)_2$, (**61**) $[Cu(L^6)(H_2O)_2](ClO_4)_2$, (**62**) $[Cu(L^6)Cl_2]$, and (**65**) $[Cd(L^6)Cl_2]$. It was observed that complexes (**62**) and (**65**), have a better inhibitory capacity against bacterial than ceftazidime (CAZ) which is more active than complexes (**60**) and (**61**) (Fig. 44) [12].

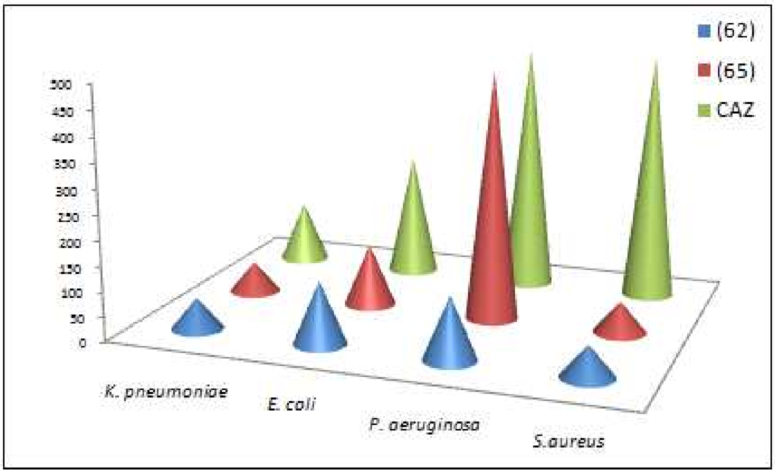

Fig. 44. The MIC values (µg/mL) of the complexes (**62**), (**65**) and ceftazidime (CAZ) against bacterial strains

The complex (**65**) is inactive against all fungal strains, but all the other studied complexes possess an activity comparable with that of fluconazole (Flcz) (Fig. 45).

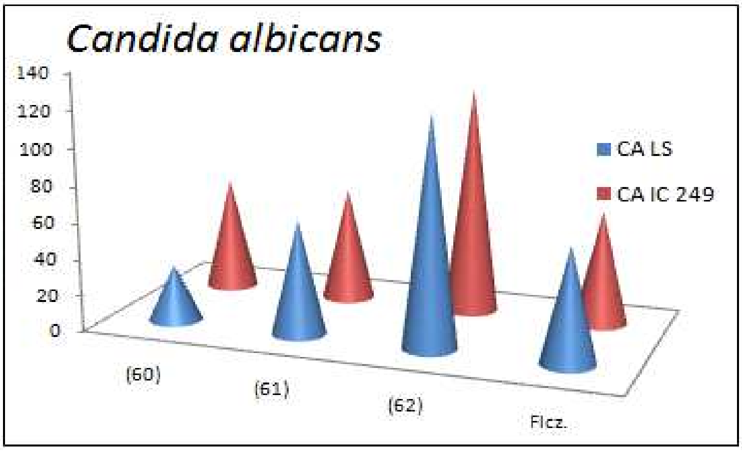

Fig. 45. The MIC values (µg/ml) of the studied complexes and of fluconazole(Flcz.) against *Candida albicans* strains

Analyzing the results obtained after measurement of the absorbance that is determined by the thickness of the microbial strains layer fixed on the support, it was observed that:

- the complexes (**60**) – (**62**) and (**65**) have a higher ability than the standard drugs to inhibit the adherence of the microbial strains to the inert substratum (Fig. 46 a and b);
- a decrease of bacterial and fungal strains adherence in the presence of tested compounds and at minimal inhibitory concentrations it was observed (Fig. 46c).

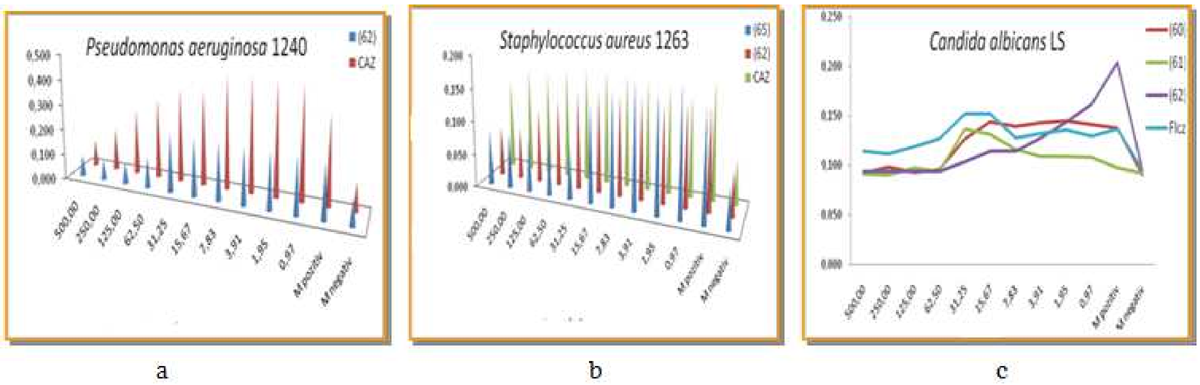

Fig. 46. The influence against the adherence of microbial species at the inert support for macrocyclic compounds (**60**) [Co(L^6)(H_2O)$_2$](ClO_4)$_2$, (**61**) [Cu(L^6)(H_2O)$_2$](ClO_4)$_2$, (**62**) [Cu(L^6)Cl_2], and (**65**) [Cd(L^6)Cl_2]

The use of the organic compounds that possess two functional groups in their molecules for synthesizing new Schiff bases, opens a large research field having in view the multiple possibilities of the ligands to be involved in coordination. Many natural organic compounds are di– or multi–functional, and the research presented in this thesis may be a starting point for investigating the natural occurring processes.

CONCLUSIONS

1. Five ligands of the azomethine class starting from difunctional products were obtained. Three of them were new ligands. In addition, four of these ligands were synthesized by the condensation reaction of *o*–tolidine and several carbonyl compounds. The fifth ligand was obtained by the condensation reaction between butanedione and 2–aminopyridine. These ligands contain as possible donor atoms azomethine N/pyridine N, phenol O/carbonyl O, and their structures was supported by the physico–chemical and spectral methods (melting points, elemental analysis, IR, UV-Vis, NMR, mass and single crystal X-ray diffraction spectra).
2. A number of 66 new complexes of Cu(II), Co(II), Ni(II), Cd(II), and Zn(II) ions were synthesized and characterized through elemental analysis, spectral analysis (IR, UV-Vis, NMR, EPR, ESI–MS), electric conductibility and magnetic susceptibility measurements, cyclic voltammetry, fluorescence, and thermal analysis. A number of 59 new complexes were obtained by using five ligands, metallic ions M(II) salts, and the other seven compounds with macrocyclic structures were synthesised by template method starting from butanedione, *o*–phenylenediamine and the salt of the metallic ion Co(II), Cu(II), Cd(II) and Zn(II).

3. In order to determine the influence of complexes on the biological properties, the synthesized substances were tested as antimicrobial agents by the determination of the MIC concentration which can prevent the growth and the development of ten standard microbial cultures. The results of these tests revealed that some ligands have a weak action against the studied bacterial strains. However, they have a strong action against fungal strains, sometimes stronger than a standard drug. After complexation, the inhibitory activity change significantly due to the presence of the metal ions and the anions; depending on the nature of the ligand, this activity can present an important increase or decrease in comparison with the activity of specific standard drugs (ceftazidime and fluconazole).
4. Other research direction was to analyze the influence of the ligands and the obtained complexes on the biofilms that was evaluated after absorbance measurement of fixed microbial strains on the inert substratum. The obtained results revealed that the ligands and some complexes inhibited the adherence on the inert support at minimal inhibitory concentrations, but also at subinhibitory concentrations; in some situations, the new complexes present a superior activity in comparison with the standard drugs.

REFERENCES

1. M. Bonilla-Alvarez, M. Palmeri, D. Davis, J. S. Fritz, *Talanta*, 34, **1987**, 473-492; N. H. Lee, J. C. Byun, J. S. Baik, C. Han, S. Han,*Bull. Korean Chem. Soc.*, 23, **2002**;1365-1366; K. G. Gupta, A. K. Sutar, Coord. *Chem.Rev*., **2007**, CCR-110833; E. Kwiatkowaski, G. Romanovki, W. Nowicki, M. Kwiatkowaski, K. Swinska, *Polyhedron*,26, **2007**, 2559-2568; G. Grivani, S. DelKhosh, K. Fejfarova, M. Dusek, A. D. Khalaji, *Inorg. Chem. Comm.*, 27, **2013**, 82-87

2. T. Roșu, E. Pahonțu, R. Georgescu, N. Stănică, G. L. Almăjan, *Polyhedron*, 29, **2010**, 757-766; A. Ourari, K. Ouari, M. A. Khan, G. Bouet, *J. Coord. Chem*., 61, **2008,** 3846-3859; B. Dede, F. Karipcin, M. Cengiz, *J. Hazard Mat*., 163, **2009,**1148–1156; J. Zhang, J. Xie, Y. Tang, J. Li, J-z. Li, W. Zeng, C-w Hu, *J. Chem. Res*., **2005,** 130-134; H. Keypour, M. Shayesteh, M. Rezaeivala, F. Chalabian, L. Valencia, *Spectrochim. Acta A: Mol. Biomol. Spectr.*, 101, **2013**, 59-66; A.Z. El-Sonbati, M.A. Diab, A.A. El-Bindary, M.I. Abou-Dobara, H.A. Seyam, *Spectrochim. Acta A: Mol. Biomol. Spectr.*,104, **2013**, 213-221

3. E. Hadjoudis, I. M. Mavridis, *Chem. Soc. Rev*., **33**, **2004,** 579-588; G. H. Brown, *Photochromism: Techniques of Chemistry*,Vol. III, Wiley-lnterscience, New York, **1971**

4. R. B. Mohod, S. G. Bhdange, A. S. Aswar, *Ind. J. Chem.*, 40, **2001**, 1110-1118

5. A. M. Ali, H. A. Ayman, T. A. Mohamed, H. M. Bassem, *J. Appl. Sci. Res.*,3(2), **2007,** 109-118; A. M. Ali, A. H. Ahmed, A. Tarek, T. A. Mohamed, B. H. Mohamed, *Trans. Met. Chem*,32, **2007**, 461-467; I. Alan, A. Kriza, C. Drăghici, L. G. Almăjan, *Rev. Chim.*,10, **2011**, 975-980

6. W. J. Geary, *Coord. Chem. Rev.*,7, **1971**, 81-82

7. K. Singh, P. Patel, B. Agarwala, *Spect. Lett.*, 28, **1995**, 751-759; K. Nakamoto, *Infrared and Raman Spectra of Inorganic and Coordination Compounds*, New York, Wiley, **1986;** G. Socrates, *Infrared and Raman characteristic group frequencies – Tables and Charts*,3rd, Ed., John Wiles & Sons, West Sussex, **2004**

8. A. P. Lever, *Inorganic Electronic Spectroscopy*, Amsterdam, London, New York, Elsevier, **1986** E. König, *Struct. Bond*., 9, **1971**, 175-212; V.P. Daniel,B. Mukuran,B.S. Kumari,K. MIhanan,*Spectrochim. Acta Part A*,70, **2008**, 403-409 ; E. Vinuelas-Zahinos, M. A. Maldonado-Rogado, F. Luna-Giles, F. J. Barros-Garcia, *Polyhedron*, 27, **2008**, 879-885

9. T. Roșu, A. Gulea, E. Pahonțu, A. Cotovaia, *Rev. Chim.*,58(5), **2007**, 475-480; B. J. Hathway, A.A.G. Tomlinson, *Coord. Chem. Rev*,5, **1970**, 1-11; N. M. El-Metwally, I. M. Gabor, A. A.Abou-Hussen, *Trans. Met. Chem.*,31, **2006**, 71-78; K. Kneubuhl, *J. Chem. Phys.*,33, **1960,** 1074–1078; B. D. Kivelson, R. Neiman, *J. Chem. Phys.*,35, **1961**, 149-154; M. J. Adam, L. D. Hall, Can. J. Chem.,60, **1982**, 2229-2237

10. A. J. Bard, L. R. Izatt, *Electrochemical Methods: Fundamentals and Applications*, 2nd Ed, New York, **2001;** B. X. Ye, Y. Xu, F. Wang, Y. Fu, M. P. Song, *Inorg. Chem. Commun*, 8, **2005**, 44-51; J. Vazquez-Arenas, I. Lazaro, I., Cruz, R., *Electrochim. Acta*,2, **2007**, 610-617

11. G. Pethe, A. Yaul, A. Aswar, *J. Therm. Anal. Calorim.*,106**, 2012,** 348-356; M. Badea, R. Olar, V. Uivarosi, D. Marinescu, V. Aldea, S. F. Barbuceanu, G. M. Nitulescu, *J. Therm. Anal. Calorim.*,105, **2011**, 559–564; C. K. Modi, D. H. Jani, *J. Therm. Anal. Calorim.*, 102**, 2010**, 1001–1010; R. Olar, M. Badea, D. Marinescu, R. Mardale, *J. Therm. Anal. Calorim.*,105**, 2011**, 553–557

12. R. M. Donland, J. Costerton, *Clinic. Microb. Rev.*, 15, **2002**, 167-193; V. Lazăr, *Aderența microbiană*, Editura Academiei Române, București, **2003;** C. Limban, A.V. Missir, I.C. Chirilă, G.M. Niculescu, C. Drăghici, M.T. Căproiu, M.C. Chifiriuc, O. Drăcea, *Rev. Chim.*, 58, **2009**, 637-642

13. I. Alan, A. Kriza, R. Olar, N. Stanica, M. Badea, *J. Therm.Anal. Calorim*.,111, **2013**, 1163-1171; I. Alan, A. Kriza, M. Badea, N. Stanica, R. Olar, *J. Therm. Anal. Calorim.*, 111, **2013**, 483-490;DOI 10.1007/s10973-012-2249-y

14. W. Henderson, J.S. McIndoe, Mass Spectrometry of Inorganic, *Coordination and Organometallic Compounds*, John Wiley & Sons, **2005**; W. A. Alves, G. Cerchiaro, A. Paduan Filho, D. M. Tomazela, M. N. Eberlin, A. M. Da Costa Ferreiro, *Inorg. Chim. Acta*, 358(13), **2005**, 3581-3591

15. M. S. Refat, N. M. El-Metwaly, *Spectrochim. Acta*, 81(1), **2011**, 215-227; J.-H. Yu, J. Lu, Y. Xu, X. Zhang, J.-Q. Xu, *Inorg. Chim. Acta*,359(10), **2006**, 3205-3211

16. F. Cimpoesu, F. Dahan, S. Ladeira, M. Ferbinteanu, J.-P. Costes, *Inorg. Chem.*, 51**,** **2012**, 11279−11293

17. I. Alan, A. Kriza, O. Drăcea, N. Stănică, *J. Serb. Chem. Soc.*,78(7), **2013**, 847-857

18. H. Aneetha, J. Padmaja, P. S. Zacharis, *Polyhedron*,15(14),**1996**,2445-2451; H-C. Wu, P. Thanasekaran, C-H Tsai, J-Y Wu, S-M Huang, Y-S Wen, K-L Lu, *Inorg. Chem.*,45, **2006**, 295-303; I. Alan, A. Kriza, O. Dracea, N. Stănică, *Internat. J.Pharm.Techn.*,4(2), **2012**, 4436-4450

19. S. K. Lim, B. H. Choi, Y. Min, D. Kim, I. Yoon, S. S. Lee, I. M. Lee, *J. Organomet. Chem.*,689, **2004**, 224-237; D. J. Otway, W. S. Rees, *Coord. Chem. Rev.*,210, **2000**, 279-328; D. H. Lee, *M. S. Thesis*, Inha University, **2004**; M. Imran, L. Mitu, S. Latif, Z. Mahmood, I. Naimat, S. Zaman, S. Fatima, *J. Serb. Chem. Soc.*,75(8), **2010,** 1075-1084

20. J. Elimes, M. Basato, G. Valle, *Inorg. Chim. Acta*, 290, **1999**, 14-20; X. Shen, L. Sun, B. K. Jiang, X. Wang, A. Nakashima, N. Miyamoto, K. Sakata, Y. Xu, D. R. Zhu, *Inorg. Chem. Comm.*,14, **2011**, 1555-1560; D. Singh, K. Kumar, R. Kumar, J. Singh, *J. Serb. Chem. Soc.*,75(2), **2010,** 217-228; D. Singh, K. Kumar, *J. Serb. Chem. Soc.*,75(4), **2010**, 475-482.

SCIENTIFIC PUBLICATIONS AND COMMUNICATIONS

(researches developed and presented in Ph.D. thesis)

ISI-QUOTED PAPERS

1. Ionela Alan, Angela Kriza, Nicolae Stanica, Constantin Draghici, Gabriela Laura Almajan, "Synthesis, Characterization and Antibacterial Activity of Co(II), and Cu(II) Complexes of N,N'-bis-(salicylidene)-o-tolidine", *Revista de Chimie,* **2011**/62(10)/975-980

2. Ionela Alan, Angela Kriza, Olguta Dracea, Nicolae Stanica "Synthesis, Characterization and Antimicrobial Activity of Some Cu(II) Complexes with N,N'-(Pyridine-2-yl-methylene)-3,3'-dimethylbenzidine Schiff Base", *International Journal of Pharmacy and Technology,* **2012**/4(2)/4436-4450

3. Ionela Alan, Angela Kriza, Olguta Dracea, Nicolae Stanica, “New Complexes of Co(II), Ni(II) and Cu(II) with the Schiff base 2,2’-[(3,3’-dimethyl[1,1’-biphenyl]-4,4’-diylbis-(nitrilomethylidyne)]bis[6-methoxyphenol]”, *Journal of the Serbian Chemical Society*, **2013**/78(7)/947-957

4. Ionela Alan, Angela Kriza, Mihaela Badea, Nicolae Stanica, Rodica Olar, “Synthesis and Characterization of Co(II), Ni(II), Zn(II) and Cd(II) Complexes with 5-bromo-*N,N’*-bis-(salicylidene)-*o*-tolidine”, *Journal of Thermal Analysis and Calorimetry*, **2013**/111/483-490

5. Ionela Alan, Angela Kriza, Rodica Olar, Nicolae Stanica, Mihaela Badea, “Spectral, Magnetic and Thermal Characterization of New Complexes with Schiff Base 5-bromo-*N,N’*-bis-(salicylidene)-*o*-tolidine”, *Journal of Thermal Analysis and Calorimetry*, **2013**/111/1163-1171.

INTERNATIONAL CONFERENCES ATTENDANCE

1. Ionela Alan, Rodica Olar, Mihaela Badea, Angela Kriza, “Thermal, Spectral and Magnetic Characterization of new Complexes with Schiff Base 5-bromo-*N,N’*-bis-(salicylidene)-*o*-tolidine”, 1st *Central and Eastern European Conference on Thermal Analysis and Calorimetry,* **7-10 September 2011**, Craiova, România/poster.

2. Ionela Alan, Rodica Olar, Mihaela Badea, Angela Kriza, “Thermal and Spectral Characterization of Co(II), Ni(II), Zn(II) and Cd(II) Complexes with 5-bromo-*N,N’*-bis-(salicylidene)-*o*-tolidine”,1st *Central and Eastern European Conference on Thermal Analysis and Calorimetry,* **7-10 September 2011**, Craiova, România/poster.

Supervisor:
Scientific Ph.D.
Prof. dr. Angela Kriza

Ph.D. student:
Ionela Stan (Alan)